

BlackCAT: A catalogue of stellar-mass black holes in X-ray transients^{★,★★}

J. M. Corral-Santana¹, J. Casares^{2,3}, T. Muñoz-Darias^{2,3}, F. E. Bauer^{1,4,5}, I. G. Martínez-Pais^{2,3}, and D. M. Russell⁶

¹ Instituto de Astrofísica, Facultad de Física, Pontificia Universidad Católica de Chile (IA-PUC), Casilla 306, Santiago 22, Chile
e-mail: jcorral@astro.puc.cl

² Instituto de Astrofísica de Canarias (IAC), Vía Láctea, s/n, 38205 La Laguna, S/C de Tenerife, Spain

³ Departamento de Astrofísica – Universidad de La Laguna (ULL), 38206 La Laguna, S/C de Tenerife, Spain

⁴ Millennium Institute of Astrophysics (MAS), Nuncio Monseñor Sótero Sanz 100, Providencia, Santiago Chile

⁵ Space Science Institute, 4750 Walnut Street, Suite 205, Boulder, Colorado 80301, USA

⁶ New York University Abu Dhabi, PO Box 129188, Abu Dhabi, UAE

Received 6 August 2015 / Accepted 24 October 2015

ABSTRACT

Aims. During the last ~50 years, the population of black hole candidates in X-ray binaries has increased considerably, with 59 Galactic objects being detected in transient low-mass X-ray binaries, as well as a few in persistent systems (including ~5 extragalactic binaries). **Methods.** We collect near-infrared, optical, and X-ray information spread over hundreds of references to study the population of black holes in X-ray transients as a whole.

Results. We present the most updated catalogue of black hole transients. This contains X-ray, optical, and near-infrared observations, together with their astrometric and dynamical properties. The catalogue provides new and useful information in both statistical and observational parameters and provides a thorough and complete overview of the black hole population in the Milky Way. Analysing the distances and spatial distribution of the observed systems, we estimate a total population of ~1300 Galactic black hole transients. This means that we have only discovered less than ~5% of the total Galactic distribution.

Key words. X-rays: binaries – stars: black holes – catalogs

1. Introduction

X-ray binaries (XRBs) are systems formed by either a neutron star (NS) or a black hole (BH), which is accreting mass from a companion donor star. Their detection began thanks to the development of space-based instrumentation in the 1960s, with the number of detections rising substantially since the implementation of all-sky monitors on board X-ray satellites, e.g. *Ginga* (1987–1991), *RXTE* (1996–2012) and, more recently, *Swift* (2004) and *MAXI* (2009). They are broadly divided into high-mass X-ray binaries (HMXBs) and low-mass X-ray binaries (LMXBs) according to the mass of the donor star. In the former, the early spectral type (O–B) massive star ($\geq 10 M_{\odot}$) mainly transfers material to the compact object through strong stellar winds. In LMXBs, on the other hand, the K–M spectral type star ($M_2 \leq 1 M_{\odot}$) fills the Roche lobe and transfers mass by Roche lobe overflow through the inner Lagrangian point (Charles & Coe 2006). In this latter case, the material forms an accretion disc around the compact object whereby material is accreted. A few XRBs are also found with intermediate mass companions of spectral types in the range B–F. It has been proposed that these so-called intermediate-mass XRBs (IMXBs) may be the

progenitors of some LMXBs through an episode of enhanced mass-transfer rate (Podsiadlowski et al. 2002).

The mass transfer rate (\dot{M}) largely determines the observational properties and gives rise to a subclassification within the LMXB class. Persistent sources are those with high accretion rates ($\dot{M} \sim 10^{-8} M_{\odot} \text{ yr}^{-1}$; Tanaka & Shibazaki 1996) and X-ray luminosities close to the Eddington limit. This high luminosity ensures that the outer parts of the accretion disc dominate the optical spectrum owing to reprocessing, and effectively hide the companion star. By contrast, transient sources are systems with low accretion rates ($\dot{M} \leq 10^{-9} M_{\odot} \text{ yr}^{-1}$; Tanaka & Shibazaki 1996) which exhibit long quiescent states and sporadic outburst episodes that are produced by thermal-viscous instabilities in the accretion disc (see Frank et al. 2002 for further explanation). During these outbursts, the brightness of the system rises to luminosities similar to those found in the persistent sources. After the outburst, transients decay back to quiescent states where they remain for most of their lifetimes. Typical recurrence times between outbursts span from years to centuries, depending on \dot{M} (Ritter & King 2002; McClintock & Remillard 2006).

Observations have revealed that ~25% of the transient LMXBs contain bursting NS (King et al. 1996a) while the rest (~75%) display X-ray spectral and/or timing properties that are characteristic of accreting black holes (hereafter we will refer to transient black hole systems as black hole transients or BHTs). In this paper we focus on the properties of Galactic BHTs since they represent the vast majority of the population of BHs. However, there are a few persistent, non-active, and extragalactic XRBs that harbour or may contain BHs.

* The complete version of this catalogue will be continuously updated at www.astro.puc.cl/BlackCAT and in the Virtual Observatory, including finding charts and data in other wavelengths.

** Tables A.1 to A.4 are also available in electronic form at the CDS via anonymous ftp to (130.79.128.5) or via <http://cdsarc.u-strasbg.fr/viz-bin/qcat?J/A+A/587/A61>

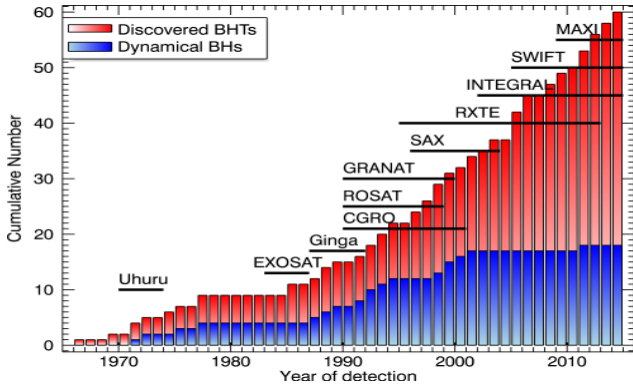


Fig. 1. Cumulative histogram of discovered (red) and dynamically confirmed (blue) BHTs as a function of time. Here, we also count *Swift* J1357.2–0933 as a dynamical BH. The lifetimes of the main X-ray satellites with all-sky monitor capabilities are shown with black lines.

Regarding the extragalactic population of BHs, dynamical evidence has been presented for LMC X-1 (a $11 \pm 1 M_{\odot}$ BH with an O7III companion; Orosz et al. 2009) LMC X-3 (a $7.0 \pm 0.6 M_{\odot}$ BH with a B3–5V star; Orosz et al. 2014 and Val-Baker et al. 2007) and M33 X-7 (a $16 \pm 1 M_{\odot}$ BH with a O7–8III star; Orosz et al. 2007) the first eclipsing stellar-mass BH ever detected.

On the other hand, indirect evidence for the presence of BHs in the HMXBs NGC 300 X-1 ($12\text{--}24 M_{\odot}$ BH with a Wolf-Rayet star, Crowther et al. 2010) and IC 10 X-1 (a $23\text{--}34 M_{\odot}$ BH with a Wolf-Rayet star, Silverman & Filippenko 2008) has been postulated. Owing to the unique challenges of observing the wind-dominated Wolf-Rayet companions, the masses of the compact objects in these systems are rather uncertain and, indeed, the presence of a neutron star cannot be ruled out (Binder et al. 2015; Laycock et al. 2015). Finally, we should also mention ultraluminous X-ray sources (ULXs), systems with X-ray luminosities that are greater than the Eddington limit for a $10 M_{\odot}$ BH. The source of these luminosities is still uncertain, and it has been proposed that they may be produced by intermediate mass BHs ($\sim 10^3 M_{\odot}$, see e.g. Miller et al. 2003) or stellar-mass BHs (e.g., Poutanen et al. 2007; Kawashima et al. 2012). More recently, for one case, it has been found that the compact object is a NS (M82 X-2; Bachetti et al. 2014) which confounds our understanding of ULXs even further.

Hereafter, we will only focus on the Galactic population of BHs. We have performed a thorough search of all X-ray systems published in literature since 1962, when the first extrasolar X-ray source was detected, (the NS system Sco X-1, Giacconi et al. 1962) up until 2015. In Sect. 2 we motivate the generation of the catalogue with a historical view of the sample of BHTs and present the catalogue itself. In Sect. 3 we study the population of BHTs, where we analyse the vertical distribution of BHTs and constrain the expected number of systems in the Milky Way. In Sect. 4 we focus on the population of dynamically confirmed BHs, presenting their distributions of periods, magnitudes, and masses.

2. BlackCAT: the catalogue of Galactic BHs

Since 1966 up to 2015, 59 BHTs have been discovered and are represented in Fig. 1 as a cumulative histogram of red bars, the slope of which represents a detection rate of ~ 1.2 targets per year. However, only 17 of these BHTs have been dynamically confirmed to harbour accreting BHs (i.e. mass function $\geq 3 M_{\odot}$,

see, e.g., Casares & Jonker 2014) and are represented by the blue bars in Fig. 1. Here, we should also add *Swift* J1357.2–0933, where the dynamical confirmation is indirect because it is not based on the detection of the secondary star. However, there is robust evidence that it contains a BH (see Corral-Santana et al. 2013 and Mata Sánchez et al. 2015 for more details).

Therefore, the 17+1 dynamical BHs represent $\sim 30\%$ of the total number of BHTs discovered so far. This low fraction is due to most BHTs becoming too faint in quiescence for radial velocity studies using current instrumentation because of their intrinsically faint companions, high extinction, large distance, or a combination of the above. This problem could be alleviated with the exquisite sensitivity of future facilities like the European Extremely Large Telescope (E-ELT), especially with better IR instrumentation. The rest of the population of BHTs are named BH candidates because they share similar X-ray characteristics in outburst to the confirmed ones, but they lack a final dynamical confirmation (see, e.g. McClintock et al. 2006 and Belloni et al. 2011 for reviews on the X-ray observational properties of the BH candidates). Indeed, NS and BH sometimes display qualitatively similar phenomenology in outburst (see, e.g. Muñoz-Darias et al. 2014) and we cannot ignore that some of the objects included in this catalogue might harbour NS.

BlackCAT is a complete catalogue containing the astrometric, photometric (near-infrared -NIR-/optical magnitudes in outburst and quiescence), number of outbursts, the peak X-ray flux, distance, finding charts, and dynamical parameters of all the BHTs discovered so far¹. In this paper we present the most relevant properties in the tables, as explained below.

We divide the catalogue into three main types of Galactic BHs: transients, persistent, and non-active, depending on their X-ray activity.

Persistent

Cyg X-1 (a $15 \pm 1 M_{\odot}$ BH with a O9.7 Iab donor star, Orosz et al. 2011a) is the only confirmed Galactic BH in a persistent X-ray binary. On the other hand, 4U 1957+11 (Wijnands et al. 2002; Nowak et al. 2008, 2012; Hakala et al. 2014) and 1E 1740.7-2942 (Sunyaev et al. 1991) are persistent BH candidates, but they have not been dynamically confirmed. GRS 1758-258 (Mandrour 1990) is a quasi-persistent microquasar with a large extinction $A_v \sim 8.4$ (Mereghetti et al. 1997) that is located near the Galactic centre region. Finally, SS 443 (Stephenson & Sanduleak 1977) is a non-transient source with a supercritical accretion regime onto a relativistic star (see Fabrika 2004 for a detailed review on the system). It is very likely a BH candidate with indirect arguments that support a compact object of $10\text{--}20 M_{\odot}$ with a high inclination (Eikenberry et al. 2001). However, despite it being intensively studied for almost 30 years, the nature of this system is still uncertain and it could be a Galactic ULX.

Non-active BHs

MWC 656 has recently been proposed as the first BH HMXB with a Be-type companion star ($3.8\text{--}6.9 M_{\odot}$ BH with a B1.5-2 III star, Casares et al. 2014). This is based on radial velocity curves of gas encircling the companion star and the spectroscopic mass of the Be star. This system has not shown any type of outbursting activity, so we label it as a non-active BH. Three other black hole

¹ The electronic and most complete version of this catalogue is available on www.astro.puc.cl/BlackCAT although all data will also be available through the Virtual Observatory.

candidates have been discovered in globular clusters: the flat-spectrum radio sources M22-VLA1 and M22-VLA2 (Strader et al. 2012) and M62-VLA1 (Chomiuk et al. 2013).

Transients

The remaining systems are transients, although some of them could be considered semi-persistents (e.g. GRS 1915+105 or 4U 1630-472) because of their long stays in the outburst state. Below, we detail the content of the tables presented in this paper. The systems included are either dynamically confirmed BHs or have shown spectra and/or timing features that are typically found in BHs (Belloni et al. 2011). We also note the existence of Cyg X-3 (Giacconi et al. 1967), a transient source showing strong radio outbursts. However, the nature of the primary, which accompanies the Wolf-Rayet donor, is unclear and it could be either an NS or a BH. Thus, we have excluded Cyg X-3 from our list of BHTs.

Table A.1 presents the basic astrometric properties of the BHTs sorted chronologically by year of detection in X-rays. The dynamically confirmed BHs are highlighted in grey. The column distribution is:

- (1) Year of discovery of the BHT;
- (2) Name of the system and optical counterpart when known;
- (3–5) Right ascension (RA) and declination (DEC) coordinates in equinox J2000. The accuracy in the astrometry and the source of the coordinates are also shown;
- (6–7) Galactic longitude (ℓ) and latitude (b) in degrees;
- (8–9) Estimated distance (d) and height above the Galactic plane (z) in kpc;
- (10) Number of outbursts detected after discovery in X-rays;
- (11) References for the detection, best coordinates, and distance determinations.

Table A.2 shows the main properties, both in outburst and in quiescence, for all the BHTs presented in Table A.1. We also list the measured or predicted orbital period. Again, the dynamically confirmed BHs are highlighted in grey. The column distribution is:

- (1) ID number used for cross-reference with the web version of this catalogue;
- (2) Name of the system and optical counterpart when known;
- (3) Peak X-ray flux in $\text{erg s}^{-1} \text{cm}^2$, standardized to the 2–10 keV band. To do so, we begin with the X-ray flux that has been published in the literature (or in archive). We assume a power-law spectrum with a photon index $\Gamma = 2$ (Belloni et al. 2011) and the total neutral Galactic Hydrogen column density (N_{H}), published by Kalberla et al. (2005). If there is a measured N_{H} published in literature derived from direct X-ray spectral analysis, we use this instead of the radio-derived interstellar one;
- (4–5) Optical or IR magnitude in the peak of the outburst and quiescence, respectively, in the AB system. To document the original observed band, we provide the name of the band in its original system;
- (6) Optical Galactic extinction $[E(B - V)]$ reported in the literature. If unknown, we list the total Galactic line-of-sight absorption given by the Schlafly & Finkbeiner (2011) dust maps;
- (7) Reported or estimated orbital period of the binary in hours;

- (8) References for all the parameters above.

Table A.3 lists the optical/NIR photometry of the dynamical BHTs in quiescence:

- (1) Preferred name of the dynamically confirmed BHT;
- (2–9) Quiescent magnitudes of the dynamically confirmed BHTs. All the magnitudes were transformed to the AB system using the transformation coefficients taken from Table 2 in Frei & Gunn (1994) and Eqs. (5) in Blanton et al. (2005). To document the original observed band, we provide the name in its original system;
- (10) References of the magnitudes.

Table A.4 provides the dynamical parameters of the BHTs:

- (1) Preferred name of the dynamically confirmed BHT;
- (2) Spectral type of the companion star;
- (3) The orbital period of the binary in hours;
- (4) The radial velocity of the companion star (K_2) in km s^{-1} ;
- (5) The mass function of the BH $f(M_1)$ in M_{\odot} ;
- (6) The mass of the BH (M_1) in M_{\odot} . If there is an uncertain value, we prefer to show a range of masses;
- (7) The binary mass ratio $q = M_2/M_1$;
- (8) The inclination of the system (i) in degrees;
- (9) The rotational broadening ($v_{\text{rot}} \sin i$) in km s^{-1} ;
- (10) References of all the parameters.

At the bottom of each table, we present a detailed list with the particularities marked in Table A.1 and Table A.2.

This census is the most updated available and, compared to previous catalogues (e.g. Gottwald et al. 1991; Chen et al. 1997; Remillard & McClintock 2006; Ritter & Kolb 2003; Liu et al. 2006, 2007), represents a substantial improvement in both statistics and observational parameters. While it only focuses on the population of BHs, it provides a thorough and more complete coverage of optical and NIR data and dynamical parameters².

3. Analysis of the spatial distribution of BHTs

Table A.1 allows us to perform a statistical study of the distribution of BHTs in the Galaxy. In Fig. 2, we plot the 35 objects with estimated distances as viewed from the pole of the Milky Way. Filled orange circles represent the dynamically confirmed BHs while yellow stars mark the BH candidates. About 50% of the confirmed BHs are located within 4.5 kpc of the Sun. This is a clear indication that interstellar extinction is a severe limitation to dynamical mass determinations. Moreover, from Fig. 2 it seems that almost all BHs lie within a spiral arm. Thus, for BHTs with uncertain distances, likely values could be estimated or constrained using the distance to the spiral arm.

Figure 3 shows the position of all the BHTs in Galactic coordinates overlaid onto a projected image of the Milky Way, as well as histograms of their distribution in Galactic longitude and latitude. There is a clear concentration of objects towards the direction of the bulge ($340^{\circ} < \ell < 20^{\circ}$ and $|b| < 10^{\circ}$, Dwek et al. 1995) and disc. Only two objects are located at high Galactic latitudes (XTEJ1118+480 at $b = +62^{\circ}$ and *Swift* J1357.2–0933 at $b = +50^{\circ}$), while three BHTs lie between $150^{\circ} < \ell < 210^{\circ}$. Moreover, 31 out of the 59 BHTs have no reported quiescent

² It is available at www.astro.puc.cl/BlackCAT and will be continuously updated with more systems and information in other spectral bands.

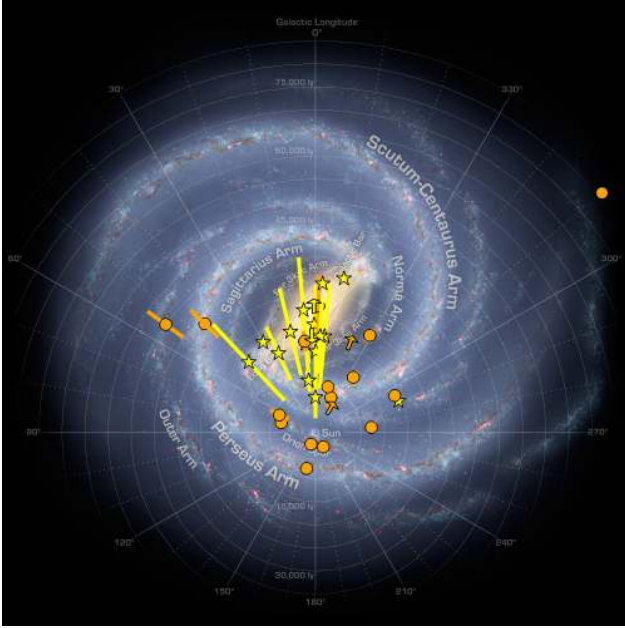


Fig. 2. Galactic distribution of 35 BHTs with distance estimates (Table A.1), as seen from the Galactic pole. Dynamically confirmed black holes are marked in orange circles, whereas BH candidates are indicated by yellow stars. Distance ranges are represented with bars while the systems with lower limits are indicated by arrows that follow the same colour index. Some systems are overlapped with other. Each faint white ring in the background image represents an additional ~ 1.5 kpc from the Sun. Objects seem to concentrate along the direction towards the Galactic centre. The dynamical BHT in the upper right of the figure is BW Cir. Background image credit: NASA/JPL-Caltech/R. Hurt (SSC/Caltech).

optical counterparts. In addition, 18 of them were detected in outburst, but they are either too faint in quiescence or the crowding of the field prevented the detection of a quiescent counterpart. On the other hand, 28 radio counterparts have been found (mostly during outburst). In Col. 5 of Table A.1, we indicate the range of the source of the coordinates together with the accuracy.

Stellar evolution predicts a population of 10^8 – 10^9 BHs in our Galaxy (van den Heuvel 2001; Remillard & McClintock 2006). However, the total number of Galactic BHTs is very uncertain and depends on several considerations. Thus, van den Heuvel (1992, 2001) estimated a population between of 500 and 1000 BHTs, based on only three to four BHTs being known at the time. Current estimates predict 10^3 – 10^4 Galactic BHTs (Romani 1998; Kiel & Hurley 2006; Yungelson et al. 2006) based on models, although these numbers are probably an underestimate because of the existence of systems with extremely long outburst duty cycles (Ritter & King 2002) or very faint peak X-ray luminosities (King & Wijnands 2006).

Here we revisit the problem of the size of the Galactic population of BHs, based on the currently observed sample, which is heavily affected by extinction. Duerbeck (1984) modelled the density distribution of several interacting binaries in the Galaxy. In a similar way, we want to obtain the density of Galactic BHTs $\rho(z)$ and analyse the height distribution (z ; Col. 8 in Table A.1). Only 35 out of the 59 detected BHTs have estimated distances. Because of their transient nature, we have only detected those systems that went into outburst. Therefore, in a given period of time, we have only discovered a fraction of them (e.g. the brightest and/or closest BHTs – with the shortest outburst cycles). Thus, to derive the true z distribution, we first need to find the

maximum radial distance at which completeness of the sample is guaranteed, i.e. such that none of the X-ray outbursts are missed.

The completeness of the sample can be obtained from the analysis of the density of objects as a function of the radial distance that is projected onto the Galactic plane (r). The latter is derived from the Galactic latitude and the distance listed in Cols. 5 and 6 of Table A.1.

Here, we have used 31 out of the 35 BHTs with a reported distance (we exclude the four systems with lower or upper limits). In addition, we consider a conservative 50% uncertainty in systems with only a rough estimate of distance. To derive the density of objects (Σ) up to a radii r , we count the number of BHTs lying in cylinders or radius r centred at the Sun and infinite height (h). However, given the large uncertainties with distance, in some cases an object could be placed in more than a single cylinder within errors. To account for this effect, for each object we randomly generate 10 000 values that assume a Gaussian distribution. Here, we naively assume the distance errors follow this sort of distribution, based on the assumption that all of the errors that went into the distance errors were Gaussian. In reality, we have no easy way of knowing this, as the values are from the literature, as determined by many groups, and in many cases are not fully documented. Thus, the final density of objects obtained in a cylinder is given by the median value of all the 10 000 Σ that were obtained in the process, with the error given by the standard deviation. The result is shown in Fig. 4 where the density is represented as a function of the radial distance and normalized to its maximum value. In this figure we find a plateau in Σ up to $r = 4$ kpc (within errors) and a decrease for $r > 4$ kpc. We interpret this as an indication that the density of objects is approximately constant with increasing radii up to ~ 4 kpc. We note here that it is difficult to establish a limit, but the density decreases clearly at $r > 4$ kpc, whereas it is not clear before this limit. Moreover, using the counting method proposed by Duerbeck (1984), we obtain a more abrupt decrease in Σ for $r > 4$ kpc. However, we believe this technique is unsuitable for systems with large uncertainties in the distance.

We also perform a complementary analysis based on the X-ray luminosity. The least luminous BHT detected is XTE J1118+480 which reached an X-ray luminosity of 3.6×10^{35} erg s $^{-1}$ in the 2–10 keV range (Dunn et al. 2010). Therefore, we can assume that no BHT peaked at a lower luminosity. The sensitivity limits by the all-sky monitor (ASM) on RXTE in the 2–10 keV range have been above 2.4×10^{-10} erg s $^{-1}$ cm $^{-2}$ since 1996, which means that any BHT that reached 3.6×10^{35} erg s $^{-1}$ within 3.5 kpc would have been detected (without considering absorption). This is consistent with the method described above and, therefore, we assume that the sample of BHTs is complete out to ~ 4 kpc.

There are ten objects in this volume (listed in Table 1). However, for the sake of the analysis we should only consider those BHTs detected since the rate of discoveries has become more or less constant. We assume that this has occurred since 1988 (see Fig. 1) when the sky started to be intensively scrutinized by all-sky monitors on-board X-ray satellites. Hence, we eliminate A0620–003 from this analysis because it was discovered in 1975 – before the beginning of the assumed constant rate of discoveries. This yields nine BHTs in the solar neighbourhood ($r \leq 4$ kpc), discovered at a rate of ~ 0.3 BHTs yr $^{-1}$ since 1988. For comparison, in the same time interval, ~ 46 BHTs have been discovered in the whole Galaxy (which implies a rate of ≈ 1.7 BHTs yr $^{-1}$).

It is expected that the vertical distribution of BHTs will follow the same exponential function as the stellar distribution

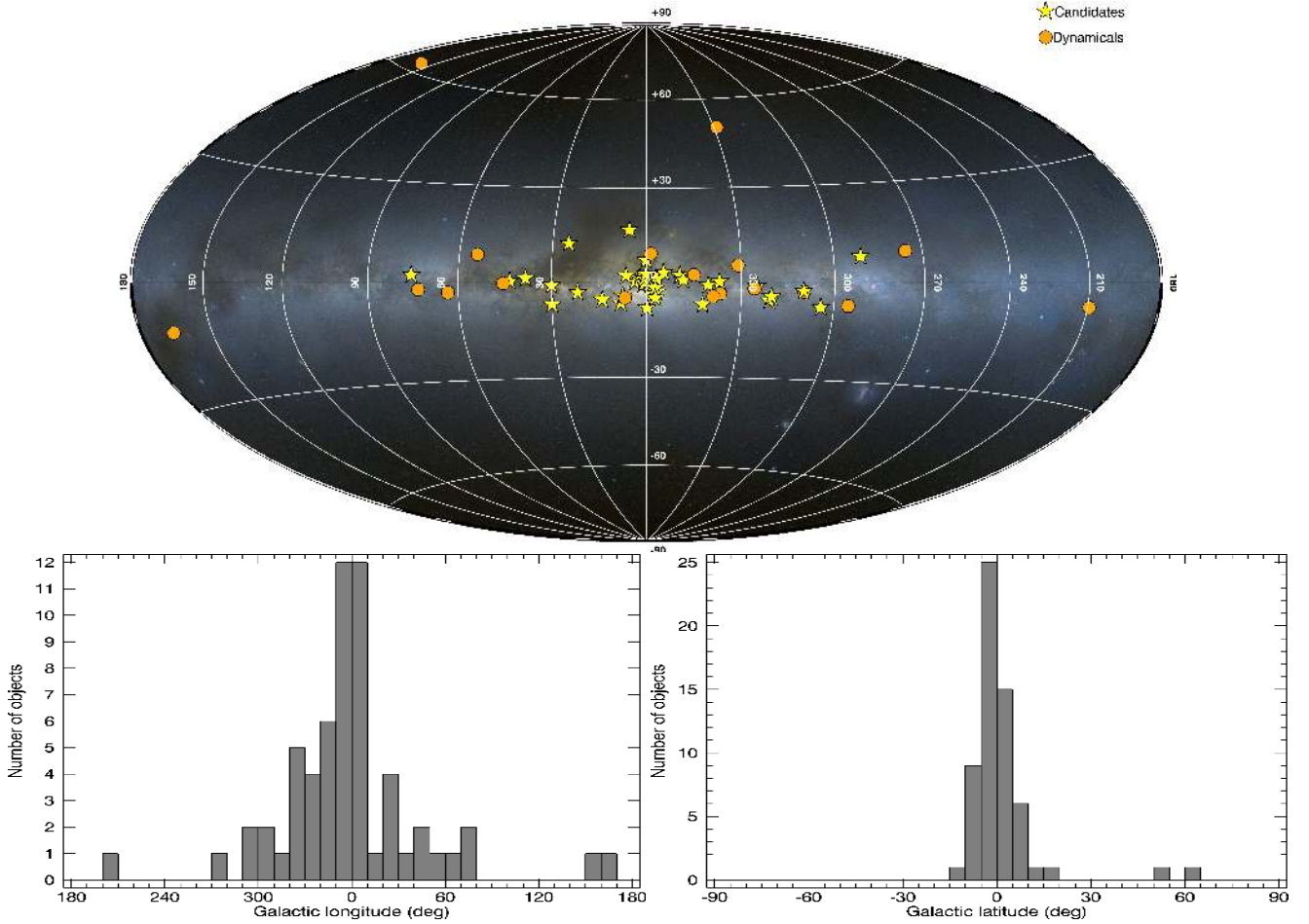


Fig. 3. *Top:* the distribution of dynamically confirmed BHs (circles) and BH candidates (stars) in the Galactic plane, using the Hammer projection. (Background image credit: Mellinger 2009). Some of the symbols are overlapped by others, especially in the Galactic centre region. *Bottom:* histogram of the distribution of BH transients in Galactic longitude (*left*) and latitude (*right*). A 10° bin size in longitude and 5° bin in latitude were used respectively.

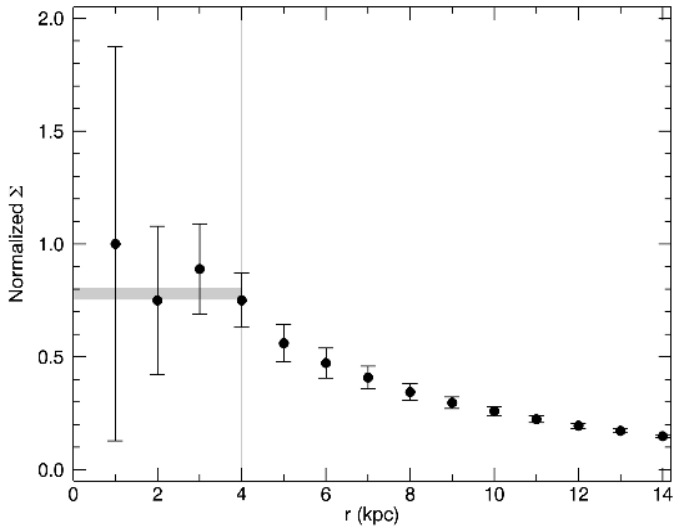


Fig. 4. Variation of the density of BHTs (Σ) in a cylindrical volume of infinite height h with increasing radii r . Above $r > 4$ kpc the density decreases and, therefore, we infer the sample of BHTs is complete out to $r \sim 4$ kpc (grey bar).

(Duerbeck 1984). In addition, it is reasonable to assume that the population of BHTs is representative of the parent Galactic

Table 1. List of BHTs within $r = 4$ kpc of completeness.

ID	Name	d (kpc)	z (kpc)	Ref.
40	XTE J1818-245	3.55 ± 0.75	-0.26 ± 0.05	Cadolle Bel et al. (2009)
33	XTE J1650-500	2.6 ± 0.7	-0.16 ± 0.04	Homan et al. (2006)
32	XTE J1118+480	1.7 ± 0.1	1.52 ± 0.09	Gelino et al. (2006)
21	GRO J1655-40	3.2 ± 0.2	0.14 ± 0.01	Hjellming & Rupen (1995)
20	GRS 1716-249	2.4 ± 0.4	0.29 ± 0.05	della Valle et al. (1994)
19	GRS 1009-45	3.8 ± 0.3	0.62 ± 0.05	Gelino (2002)
17	GRO J0422+32	2.5 ± 0.3	-0.51 ± 0.06	Gelino & Harrison (2003)
15	GS 2023+338	2.4 ± 0.1	-0.09 ± 0.01	Miller-Jones et al. (2009)
13	GS 2000+251	2.7 ± 0.7	-0.14 ± 0.04	Jonker & Nelemans (2004)
7	A0620-003	1.1 ± 0.1	-0.11 ± 0.01	Cantrell et al. (2010)

population of BHTs, since there is no strong bias against their detection in X-rays (Özel et al. 2010).

Therefore, the space/time density distribution can be approximated by

$$\rho^*(z) = \rho_0^* \exp\left(\frac{-|z|}{z_0}\right) (\text{kpc}^{-3} \text{ yr}^{-1}), \quad (1)$$

where ρ_0^* is the space/time density of objects in the Galactic plane and z_0 the scale height of the distribution that is perpendicular to the plane of the Galaxy, both measured in the solar neighbourhood.

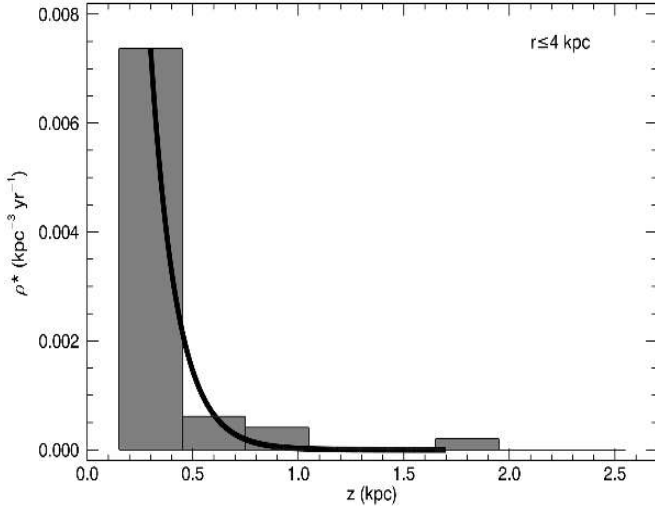


Fig. 5. Variation of the space/time density (ρ^*) of BHTs with the scale above the Galactic plane z . The solid line represents the Levenberg-Marquardt least-squares fit (Markwardt 2009) to the exponential function shown in Eq. (1).

Using a Levenberg-Marquardt non-linear least-squares fit (Markwardt 2009) of $\rho(z)$, we derive $\rho_0^* = 0.08 \pm 0.01 \text{ kpc}^{-3} \text{ yr}^{-1}$ and $z_0 = 0.123 \pm 0.008 \text{ kpc}$ (see Fig. 5). This small scale height z_0 indicates a clear concentration of systems in the plane.

To obtain the final space density of BHTs $\rho(z)$, we must assume a mean outburst recurrence period (ORP). We have only observed transients for ~ 50 years and the observed ORPs for scrutinising the X-ray sky are thus biased by this limited time frame. In Fig. 6 we show the frequency of outbursts of all the BHTs over the past 50 years. The majority of systems have shown only one outburst, with only a small fraction showing multiple outbursts. The most extreme cases are H 1743-322, GX 339-4, and 4U 1630-472, which have triggered 10, ~ 19 , and ~ 20 outbursts in ≈ 50 years (some of them were not considered “full outbursts”), respectively. In particular, 4U 1630-472 shows an ORP of 600–700 d, which lasted from 100–200 d up to 2.4 years (see, e.g. Kuulkers et al. 1997). There is also evidence for additional outbursts produced by A 0620+003 (in 1917, Eachus et al. 1976) and V404 Cyg (in 1938 and 1956, Wachmann 1948; Richter 1989) detected by analysing photographic plates that were made previous to their discoveries. Nevertheless, we included only those outbursts discovered by X-ray satellites (i.e. since 1966) to be consistent and consequently, the observed ORP is biased by the ≈ 50 yr time lapse of X-ray astronomy observations. On the other hand, based on an analysis of the mass-transfer rate needed to reach the critical surface density that produces instabilities in the accretion disc, White & van Paradijs (1996) consider it that BHTs have average ORPs above 100 yr. Therefore, the local density at the Galactic plane becomes $\rho_0 = \text{ORP} \rho_0^* = 8 \pm 1 \left(\frac{\text{ORP}}{100 \text{ yr}} \right) \text{ kpc}^{-3}$.

A rough extrapolation of this local density distribution to the entire Galaxy, assuming no radial dependence, enables us to obtain the total number of BHTs by integrating Eq. (1) in cylindrical coordinates. Using $R = 14 \text{ kpc}$ as the truncation radius for the Galactic disc and $H = 2.5 \text{ kpc}$ as the maximum height above the Galactic plane given by MAXI J1659–152 (Kuulkers et al. 2013), we find a total number of $N = 1280 \pm 120 \left(\frac{\text{ORP}}{100 \text{ yr}} \right)$ BHTs in the Galaxy with comparable properties to the systems detected so far, i.e. with peak X-ray luminosities a few tenths of the Eddington luminosity. This is consistent with the results

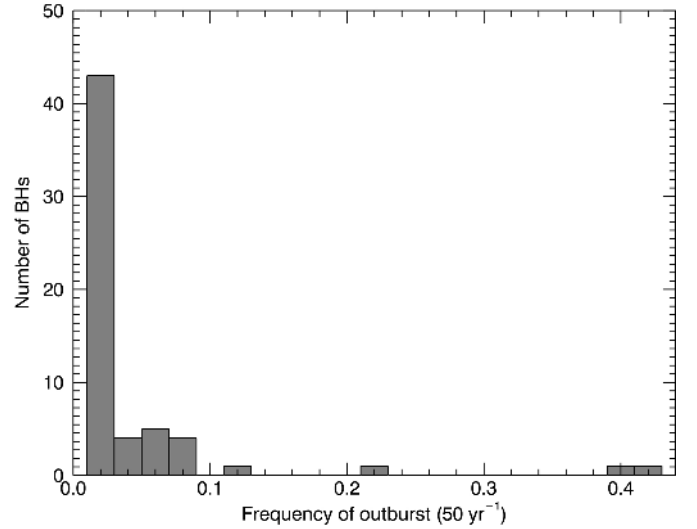


Fig. 6. Histogram of the frequency of outbursts detected over 50-yr period for all BHTs.

obtained using other techniques (van den Heuvel 1992; Tanaka 1992; White & van Paradijs 1996; Romani 1998) and implies that only $\sim 4\%$ of Galactic BHTs have been discovered.

Our empirical estimate is an order of magnitude lower than the 10^4 BHTs predicted by Kiel & Hurley (2006) or Yungelson et al. (2006) using population synthesis models. However, we note that our analysis is based on the study of observed systems but limited only to the nine BHTs with reliable distance estimates, which are located in a cylinder of 4 kpc radius centred on the Sun. In addition, we have assumed that the solar vertical distribution (ρ_0, z_0) can be extrapolated to other regions of the Galaxy. However, the bulge contains $\sim 30\%$ of the stellar mass of the Galaxy, which is confined in a reduced spheroid and it is expected to host a higher concentration of BHTs (Muno et al. 2005). Furthermore, we considered a cylinder with a height defined by MAXI J1659–152 (the object with the highest h) but there could be objects located at higher distances over the plane. Finally, we normalized our estimated value to an average recurrence period of 100 yr, which explicitly does not take into consideration any systems with lower accretion rates or longer recurrence periods, nor does it account for a likely population of intrinsically faint X-ray BHTs. Taking in all of the above, we conclude that our crude calculation of the number of BHTs expected in the Galaxy is very conservative and sets a lower limit to the hidden population.

4. Physical properties of dynamical BHTs

With the information on the apparent quiescent magnitudes, distances, and reddening listed in Tables A.1–A.4, we can recover the R -band absolute magnitudes (corrected for extinction and in the AB system) of the BHTs in quiescence. The magnitude distribution (Fig. 7, left) peaks strongly at $M_R \approx 4$ –6, where $\sim 40\%$ of the systems lie. This result is expected since the quiescent spectra are mainly dominated by the light from the donor (mostly K-type stars) with some contribution from the accretion flow (typically $\leq 50\%$ in this waveband). From Table A.4, we note a small fraction of IMXBs with A–F spectral-type companions (V4641 Sgr, 4U J1543–475, and GRO J1655–40), which have been indicated in black in Fig. 7.

In addition, from Table A.2 we can revisit the observed distribution of orbital periods that shows a bimodal shape with a

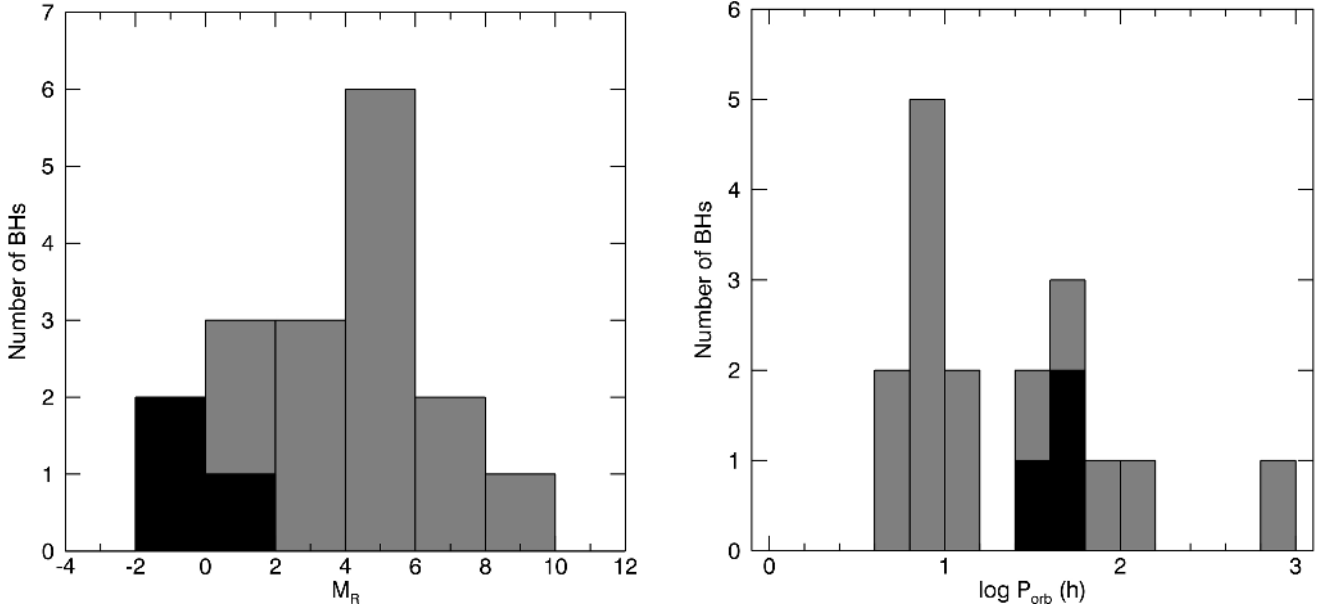


Fig. 7. Histograms of the 17 dynamically confirmed BHs. *Left:* extinction-corrected absolute R -band magnitudes in bins of 2 mag. The black histogram denotes confirmed IMXBs. *Right:* orbital periods in a logarithmic scale using bins of 0.2.

gap at ~ 15 h, known as the bifurcation period (Fig. 7, right). This is driven by different evolutionary paths, with systems above the gap evolving towards longer orbital periods through nuclear evolution of the donor stars, while angular momentum losses shrink the orbit of the binaries below the gap (Pylyser & Savonije 1988; Menou et al. 1999). In this case, the IMXBs are located at long orbital periods, consistent with the presence of giant/subgiant donor stars. The majority of systems have periods between 6–10 h, which corresponds to main-sequence or slightly evolved K-type donors filling their Roche lobes.

It is noticeable that none of the 59 BHTs listed in Tables A.1 and A.2 present X-ray or optical eclipses (the extragalactic BH-HMXB M33 X-7 is the only one known as showing eclipses). In fact, all the dynamical BHTs found so far have binary inclinations $\lesssim 75^\circ$ (see Table A.4). However, it is expected that at least 20% of the 17 dynamically confirmed BHs will have $i > 75^\circ$, taking an isotropic distribution of inclinations into consideration. Therefore, our estimate of the expected distribution of BHTs may be underestimated by 20% and should be $N \sim 1600 \left(\frac{ORP}{100\text{yr}} \right)$, although this percentage is probably smaller than the uncertainty associated with our systematic errors. Narayan & McClintock (2005) propose that the lack of high inclination systems is due to a selection effect, which is produced by the inner accretion disc hiding or obscuring the central BH, making these systems very faint in X-rays and preventing their detection during outbursts. For typical disc-flaring angles of $\sim 12^\circ$ (de Jong et al. 1996), the outer disc rim will obscure the central X-ray source permanently when viewed at inclinations $\geq 78^\circ$.

Swift J1357.2–0933 may be the first object to be seen edge-on according to the optical properties that were displayed during the decay from its 2011 outburst (Corral-Santana et al. 2013), but it did not show either X-ray or optical eclipses. Armas Padilla et al. (2014) and Torres et al. (2015) present alternative explanations to the high inclination that is based on the quiescent X-ray properties and the Hydrogen column density obtained from the Na doublet in outburst, respectively. However, Mata Sánchez et al. (2015) present new evidence that supports the edge-on configuration.

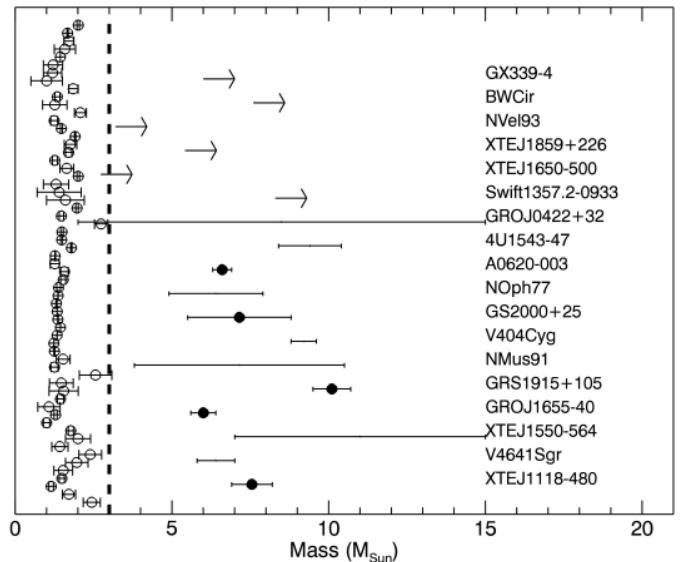


Fig. 8. Distribution of observed compact object masses. The vertical dashed line represents the maximum mass allowed for NS (Fryer & Kalogera 2001). Open circles below that limit represent the masses of the NS compiled by Lattimer & Prakash (2005), extended with updated data from Özel et al. (2012) and Antoniadis et al. (2013). The solid circles indicate reliable BH masses (adopting the values favoured by Casares & Jonker 2014), while arrows indicate lower limits based on mass functions and upper limits to the inclination.

An accurate determination of the binary inclination is crucial for obtaining the mass of the compact object. The mass distribution of black holes has a significant impact on the physics of supernova explosions, the survival of interacting close binaries and the equation of state of nuclear matter. The distribution of masses of compact objects is expected to be smooth because of its correlation with the distribution of their progenitor masses (Fryer & Kalogera 2001). However, the observed distribution shows a gap between neutron stars and BHs between 2–5 M_\odot (Fig. 8). Unlike Özel et al. (2010, 2012), here we only show with solid

circles those systems with the most reliable mass determinations following Casares & Jonker (2014). On the contrary, for those systems with inaccurate masses, we prefer to display large bars which encompass both the minimum and maximum published masses.

The existence of this mass gap is under debate. Özel et al. (2010) argue that selection effects may bias the observed distribution at high BH masses ($\geq 10 M_{\odot}$) but cannot explain the gap that may be related to the physics of supernova explosions. Farr et al. (2011) perform a Bayesian analysis of the BH mass distribution and conclude that their larger sample provides strong evidence for the existence of the gap, reinforcing the results by Bailyn et al. (1998) and Özel et al. (2010). However, Kreidberg et al. (2012) warn about a large source of systematic errors that arise from a possible underestimation of the inclination angle i . This is produced by assuming that the emission from the accretion disc (i.e. the disc veiling) is negligible in the infrared when performing ellipsoidal modelling. They found that, in the case of A0620–003, this led to an underestimate of the inclination angle of at least 10° . Because of the cubic dependence of the mass function with $\sin i$, this could lead to a considerable overestimate of the BH mass. Correcting the BH mass in GRO J0422+32 from the estimated bias in the inclination, Kreidberg et al. (2012) find that the BH would lie in the gap. However, they also note that if this object is excluded from the analysis, previous conclusions remain intact.

On the other hand, Belczynski et al. (2012) and Fryer et al. (2012) state that the mass gap may be real and it could reveal new insights into the supernovae explosion models. More recently, Kochanek (2014) suggest an alternative explanation that is based on the absence of red supergiants in the range $16.5\text{--}25 M_{\odot}$ as progenitors of type IIp supernova. As a result of the weakly bound hydrogen envelopes on these massive stars, they eject the outer layers, which leaves a BH with the mass of the star's helium core ($5\text{--}8 M_{\odot}$). This would explain (i) the lack of supernova progenitors in the $16\text{--}25 M_{\odot}$ mass range and (ii) the existence of the mass gap and the typical masses of BHs.

5. Conclusions

We have presented the main properties of a large catalogue of BHTs. Of the 59 BHTs detected in outburst so far, only $\sim 30\%$ have been confirmed as dynamical BHTs. A number of them (35) have distance estimates that allow us to study the Galactic distribution. This in turn results in a population of $\sim 1280 \left(\frac{ORP}{100 \text{ yr}}\right)$ such systems in the Milky Way. This value agrees with previous estimates that use other techniques but is an order of magnitude lower than theoretical predictions, which are based on population synthesis models. We argue that this value must be considered as a lower limit since it is based on the extrapolation of a small number of systems (nine out of the 59 systems detected so far).

We provide several tables listing the astrometric parameters, distances, number of eruptions, X-ray fluxes at the peak of the outburst and an outburst and a quiescence magnitude, reddening, and orbital periods. For dynamically confirmed systems, we have also detailed the magnitudes in quiescence in every available optical and NIR band, together with their dynamical parameters. In the online version of the catalogue, we have also added finding charts, links to the references and relevant information for forthcoming observations of these systems. We plan to include more information on other wavelengths in the near future

(e.g. radio or X-ray states) and update the online catalogue with new targets once discovered.

Acknowledgements. We thank the anonymous referee for useful comments. We acknowledge financial support from CONICYT-Chile grants FONDECYT Postdoctoral Fellowship 3140310 (JMC-S), FONDECYT 1141218 (FEB), Basal-CATA PFB-06/2007 (JMS-C, FEB), “EMBIGGEN” Anillo ACT1101 (FEB), the Ministry of Economy, Development, and Tourism’s Millennium Science Initiative through grant IC120009, awarded to The Millennium Institute of Astrophysics, MAS (FEB) and the Spanish Ministerio de Economía y Competitividad (MINECO) under grant AYA 2013-42627 (JC, TMD, IGMP). T.M.D. acknowledges hospitality during his 2015 visit to IA-PUC. This work makes use of observations from the LCOGT network, the CNTAC programs ID CN2014B-44 and CN2015A-88, the ESO Science Archive Facility under request number jcorral-160882, the GTC Public Archive at CAB (INTA-CSIC), and the Isaac Newton Group archive, which is maintained as part as the CASU Astronomical Data Centre at the Institute of Astronomy, Cambridge and the LCOGT Archive, which is operated by the California Institute of Technology, under contract with the Las Cumbres Observatory. We are thankful to Danny Steeghs and Manuel A. P. Torres for providing us with some of the finding charts and Jorge Andrés Pérez Prieto for his help with the creation of the web. We have used the web applications of the FTTOOLS (Blackburn 1995) and PIMMS (Mukai 1993) software to create the transformation of the X-ray fluxes. Some peak X-ray fluxes were provided by the ASM/RXTE teams at MIT and at the RXTE SOF and GOF at NASA’s GSFC. This research made use of the MAXI data provided by RIKEN, JAXA and the MAXI team (Matsuoka et al. 2009).

References

- Altamirano, D., Belloni, T., Linares, M., et al. 2011, *ApJ*, 742, L17
 Altamirano, D., Wijnands, R., Heinke, C. O., & Bahramian, A. 2014, *ATel*, 6469, 1
 Angelini, L., & White, N. E. 2003, *ApJ*, 586, L71
 Antoniadis, J., Freire, P. C. C., Wex, N., et al. 2013, *Science*, 340, 448
 Armas Padilla, M., Degenaar, N., Russell, D. M., & Wijnands, R. 2013, *MNRAS*, 428, 3083
 Armas Padilla, M., Wijnands, R., Degenaar, N., et al. 2014, *MNRAS*, 444, 902
 Augusteijn, T., Coe, M., & Groot, P. 2001a, *IAU Circ.*, 7710, 2
 Augusteijn, T., Kuulkers, E., & van Kerkwijk, M. H. 2001b, *A&A*, 375, 447
 Bachetti, M., Harrison, F. A., Walton, D. J., et al. 2014, *Nature*, 514, 202
 Bailyn, C. D., Orosz, J. A., Girard, T. M., et al. 1995, *Nature*, 374, 701
 Bailyn, C. D., Jain, R. K., Coppi, P., & Orosz, J. A. 1998, *ApJ*, 499, 367
 Ballet, J., Denis, M., Gilfanov, M., et al. 1993, *IAU Circ.*, 5874, 1
 Barret, D., Roques, J. P., Mandrou, P., et al. 1992, *ApJ*, 392, L19
 Barthelmy, S. D., D’Ai, A., D’Avanzo, P., et al. 2015, *GCN Circ.*, 17929, 1
 Beekman, G., Shahbaz, T., Naylor, T., & Charles, P. A. 1996, *MNRAS*, 281, L1
 Beekman, G., Shahbaz, T., Naylor, T., et al. 1997, *MNRAS*, 290, 303
 Beer, M. E., & Podsiadlowski, P. 2002, *MNRAS*, 331, 551
 Belczynski, K., Wiktorowicz, G., Fryer, C. L., Holz, D. E., & Kalogera, V. 2012, *ApJ*, 757, 91
 Belloni, T., Colombo, A. P., Homan, J., Campana, S., & van der Klis, M. 2002, *A&A*, 390, 199
 Belloni, T. M., Motta, S. E., & Muñoz-Darias, T. 2011, *BASI*, 39, 409
 Binder, B., Gross, J., Williams, B. F., & Simons, D. 2015, *MNRAS*, 451, 4471
 Blackburn, J. K. 1995, in *Astronomical Data Analysis Software and Systems IV*, eds. R. A. Shaw, H. E. Payne, & J. J. E. Hayes, *ASP Conf. Ser.*, 77, 367
 Blanton, M. R., Schlegel, D. J., Strauss, M. A., et al. 2005, *AJ*, 129, 2562
 Boer, M., Greiner, J., & Motch, C. 1996, *A&A*, 305, 835
 Borozdin, K., Sunyaev, R., & Arefiev, V. 1993, *IAU Circ.*, 5878, 1
 Borozdin, K., Alexandrovich, N., Arefiev, V., et al. 1994, *IAU Circ.*, 6083, 1
 Borozdin, K. N., Aleksandrovich, N. L., Aref’ev, V. A., Syunyaev, R. A., & Skinner, G. K. 1995, *Astron. Lett.*, 21, 212
 Bradt, H. V. D., & McClintock, J. E. 1983, *ARA&A*, 21, 13
 Brandt, S., Castro-Tirado, A. J., Lund, N., et al. 1992, *A&A*, 254, L39
 Brocksopp, C., Jonker, P. G., Fender, R. P., et al. 2001, *MNRAS*, 323, 517
 Brocksopp, C., McGowan, K. E., Krimm, H., et al. 2006, *MNRAS*, 365, 1203
 Brocksopp, C., Jonker, P. G., Maitra, D., et al. 2010, *MNRAS*, 404, 908
 Buxton, M. M., & Bailyn, C. D. 2004, *ApJ*, 615, 880
 Buxton, M., Sood, R., Rayner, D., et al. 1998, *IAU Circ.*, 6827, 1
 Buxton, M. M., Bailyn, C. D., Capelo, H. L., et al. 2012, *AJ*, 143, 130
 Cadolle Bel, M., Ribó, M., Rodríguez, J., et al. 2007, *ApJ*, 659, 549
 Cadolle Bel, M., Prat, L., Rodríguez, J., et al. 2009, *A&A*, 501, 1
 Callanan, P. J., & Charles, P. A. 1991, *MNRAS*, 249, 573
 Callanan, P. J., McCarthy, J. F., & García, M. R. 2000, *A&A*, 355, 1049
 Calvelo, D. E., Tzioumis, T., Corbel, S., Brocksopp, C., & Fender, R. P. 2009a, *ATel*, 2135, 1
 Calvelo, D. E., Vrtilik, S. D., Steeghs, D., et al. 2009b, *MNRAS*, 399, 539

- Torres, M. A. P., Jonker, P. G., Steeghs, D., & Mulchaey, J. S. 2011, [ATel](#), **3150**, 1
- Torres, M. A. P., Jonker, P. G., Miller-Jones, J. C. A., et al. 2015, [MNRAS](#), **450**, 4292
- Tsunemi, H., Kitamoto, S., Okamura, S., & Roussel-Dupre, D. 1989, [ApJ](#), **337**, L81
- Turler, M., Cadolle Bel, M., Diehl, R., et al. 2005, [ATel](#), **624**, 1
- Ueda, Y., Dotani, T., Uno, S., et al. 1997, [IAU Circ.](#), **6627**, 2
- Usui, R., Nakahira, S., Tomida, H., et al. 2012, [ATel](#), **4140**, 1
- Val-Baker, A. K. F., Norton, A. J., & Negueruela, I. 2007, in *The Multicolored Landscape of Compact Objects and Their Explosive Origins*, eds. T. di Salvo, G. L. Israel, L. Piersant, et al., [AIP Conf. Ser.](#), **924**, 530
- van den Heuvel, E. P. J. 1992, in *X-ray Binaries and Recycled Pulsars* (Kluwer Academic Publishers), 233
- van den Heuvel, E. P. J. 2001, in *Evolution of Binary and Multiple Star Systems*, eds. P. Podsiadlowski, S. Rappaport, A. R. King, F. D'Antona, & L. Burderi, [ASP Conf. Ser.](#), **229**, 525
- van der Hooft, F., Heemskerk, M. H. M., Alberts, F., & van Paradijs, J. 1998, [A&A](#), **329**, 538
- Vargas, M., Goldwurm, A., Paul, J., et al. 1996, [A&A](#), **313**, 828
- Voges, W., Aschenbach, B., Boller, T., et al. 1999, [A&A](#), **349**, 389
- Wachmann, A. A. 1948 (Berlin: Akademie-Verlag)
- Wachter, S., & Smale, A. P. 1998, [ApJ](#), **496**, L21
- Wagner, R. M., & Starrfield, S. 2002, [ATel](#), **86**, 1
- Wagner, R. M., Henden, A. A., Bertram, R., & Starrfield, S. G. 1988, [IAU Circ.](#), **4600**, 2
- Wagner, R. M., Bertram, R., Starrfield, S. G., & Shrader, C. R. 1992, [IAU Circ.](#), **5589**, 1
- Wang, X., & Wang, Z. 2014, [ApJ](#), **788**, 184
- Wang, Z., Baganoff, F. K., Muno, M., et al. 2006, [ATel](#), **935**, 1
- Warwick, R. S., Marshall, N., Fraser, G. W., et al. 1981, [MNRAS](#), **197**, 865
- Watson, M. G., Ricketts, M. J., & Griffiths, R. E. 1978, [ApJ](#), **221**, L69
- Webb, N. A., Naylor, T., Ioannou, Z., Charles, P. A., & Shahbaz, T. 2000, [MNRAS](#), **317**, 528
- White, N. E., & Marshall, F. E. 1983, [IAU Circ.](#), **3806**, 2
- White, N. E., & van Paradijs, J. 1996, [ApJ](#), **473**, L25
- White, N. E., Parmar, A. N., Sztajno, M., et al. 1984, [ApJ](#), **283**, L9
- Wijnands, R., & Miller, J. M. 2002, [ApJ](#), **564**, 974
- Wijnands, R., Miller, J. M., & van der Klis, M. 2002, [MNRAS](#), **331**, 60
- Wood, A., Smith, D. A., Marshall, F. E., & Swank, J. 1999, [IAU Circ.](#), **7274**, 1
- Woods, P. M., Kouveliotou, C., Finger, M. H., et al. 2002, [IAU Circ.](#), **7856**, 1
- Wu, K., Soria, R., Campbell-Wilson, D., et al. 2002, [ApJ](#), **565**, 1161
- Wu, J., Orosz, J. A., McClintock, J. E., et al. 2015, [ApJ](#), **806**, 92
- Yamauchi, S., & Nakamura, E. 2004, [PASJ](#), **56**, 803
- Yang, Y. J., Kong, A. K. H., Russell, D. M., Lewis, F., & Wijnands, R. 2012, [MNRAS](#), **427**, 2876
- Yungelson, L. R., Lasota, J.-P., Nelemans, G., et al. 2006, [A&A](#), **454**, 559
- Zdziarski, A. A. 2014, [MNRAS](#), **444**, 1113
- Zhang, S. N., Wilson, C. A., Harmon, B. A., et al. 1994, [IAU Circ.](#), **6046**, 1
- Zurita, C., Sánchez-Fernández, C., Casares, J., et al. 2002, [MNRAS](#), **334**, 999
- Zurita, C., Casares, J., Hynes, R. I., et al. 2004, [MNRAS](#), **352**, 877
- Zurita, C., Rodríguez, D., Rodríguez-Gil, P., et al. 2005, [ATel](#), **383**, 1
- Zurita, C., Corral-Santana, J. M., & Casares, J. 2015, [MNRAS](#), **454**, 3351
- Życki, P. T., Done, C., & Smith, D. A. 1999, [MNRAS](#), **309**, 561

Appendix A: Tables of BHTs

Table A.1. Astrometric properties.

(1) Year	(2) Name	(3) RA (h m s)	(4) Dec ($^{\circ}$ ' '')	(5) Error ^a ''/(s. '')	(6) ℓ ($^{\circ}$)	(7) b ($^{\circ}$)	(8) d (kpc)	(9) z (kpc)	(10) Outb.	(11) Ref.
2014	IGR J17454-2919 ¹	17 45 27.69	-29 19 53.83	x 0.6	359.6444	-00.1765				Chenevez et al. (2014a), Paizis et al. (2015)
	IGR J17451-3022 ²	17 45 06.72	-30 22 43.30	x 0.6	358.7115	-00.6580				Chenevez et al. (2014c), Chakraborty et al. (2014)
2013	MAXI J1828-249	18 28 58.07	-25 01 45.88	o 0.03	008.1145	-06.5458				Nakahira et al. (2013), Kennea et al. (2013)
	SWIFT J1753.7-2544	17 53 39.85	-25 45 14.20	i 0.3	003.6476	+00.1036				Krimm et al. (2013), Rau et al. (2013a)
	SWIFT J174510.8-262411	17 45 10.85	-26 24 12.60	r (0.001,0.01)	002.1107	+01.4034	<7*	<0.17		Cummings et al. (2012), Miller-Jones & Sivakoff (2012)
2012	SWIFT J1910.2-0546 (MAXI J1910-057)	19 10 22.80	-05 47 55.92	o 0.3	029.9026	-06.8440				Muñoz-Darias et al. (2013)
	MAXI J1305-704	13 06 55.30	-70 27 05.11	r (0.003,0.07)	304.2375	-07.6177				Krimm et al. (2012), Usui et al. (2012), Rau et al. (2012)
2011	MAXI J1836-194 ³	18 35 43.44	-19 19 10.48	e (0.00003,0.0002)	013.9456	-05.3542	7 \pm 3	-0.70 \pm 0.30		Sato et al. (2012), Coniat et al. (2012)
	MAXI J1543-564 ⁴	15 43 17.18	-56 24 49.61	r (0.049,0.775)	325.0855	-01.1214				Negoro et al. (2011b), Russell et al. (2014, 2015)
	SWIFT J1357.2-0933⁵	13 57 16.82	-09 32 38.55	oi 0.3	328.7019	+50.0042	>2.29	>1.75		Negoro et al. (2011a), Miller-Jones et al. (2011b)
2010	MAXI J1659-152	16 59 01.68	-15 15 28.73	e 0.0001	005.5003	+16.5167	8.60 \pm 3.70	2.44 \pm 1.05		Krimm et al. (2011b), Rau et al. (2011b), Mata Sánchez et al. (2015)
2009	XTE J1752-223	17 52 15.09	-22 20 32.36	e 0.0014	006.4231	+02.1143	6 \pm 2	0.22 \pm 0.07		Negoro et al. (2010), Paragi et al. (2010), Kuulkers et al. (2013)
	XTE J1652-453 ⁶	16 52 20.33	-45 20 39.99	r 0.32	340.5297	-00.7867				Markwardt et al. (2009b), Miller-Jones et al. (2011a), Raiti et al. (2012)

Notes. Columns: (1) Year of detection; (2) Name (and counterpart name); (3–5) RA–Dec coordinates (J2000), error in astrometry and source of the coordinates^(†); (6–7) Galactic longitude and latitude, respectively; (8–9) distance from Sun and above the Galactic plane; (10) number of outbursts reported after the discovery outburst and (11) references for detection, coordinates and distance. **In this catalogue we have included all the BH candidates detected so far. Dynamical BHs are highlighted in grey boxes.** (†) In column 5, the letter preceding the error value indicate the source of the coordinates: radio (r), interferometry in radio (e), optical (o), infrared (i), X-rays (x) or a combination of them. In case of different errors in RA and DEC (respectively), both are shown in parenthesis. (†) These values are uncertain estimates. (1) IGR J17454-2919: the nature of this transient source is still unclear. Paizis et al. (2015) has proposed that 2MASS J17452768-2919534 is the IR counterpart although it is 2.4" away from the X-ray position. (2) IGR J17451-3022 has shown periodicity in its light curve of ~ 6.3 h (Jaisawal et al. 2015) which would imply a $>70^{\circ}$ inclination. However the nature of the compact object is still unclear and it might be a magnetar (Heinke et al. 2014). (3) MAXI J1836-194: there is a field star 0.37" away from the position of the BH candidate (Russell et al. 2014). (4) MAXI J1543-564 has no clear counterpart in optical/IR. Rau et al. (2011a) reported 3 possible objects close or within the radio (Miller-Jones et al. 2011b) and X-ray (Kennea et al. 2013; Mata Sánchez et al. 2015). The distance is still uncertain (see Rau et al. 2011b; Shahbaz et al. 2013; Mata Sánchez et al. 2015). (6) XTE J1652-453 has no clear counterpart in IR and there are doubts between close objects. (7) Swift J174540.2-290005 is 1 pc from Sgr A* assuming an 8.5 kpc distance (Kennea et al. 2006b). If this transient is an X-ray binary it would be a LMXB (Wang et al. 2006). (8) IGR J17497-2821 seems to be blended with a bright star SE of the target (Torres et al. 2006a). Probably located in the Galactic bulge. (9) Swift J1753.5-0127 remains in a low/hard X-ray state since its outburst in 2005. (10) IGR J17091-3624 showed outbursts in 2007 (Capitaino et al. 2009) and 2011 (Krimm et al. 2011a). Re-examination of archival data showed that it was also active in 1994, 1996 and 2001 (Revnivisev et al. 2003; in 't Zand et al. 2003; Capitaino et al. 2006). (11) XTE J1118+480 showed an outburst in 2005 (Zurita et al. 2005). (12) XTE J2012+381 is blended with a star at 1.1" (Hynes et al. 1999). (13) XTE J1748-288 showed hard spectrum. No counterpart has been found. An unresolved radio source was detected (Hjelleim et al. 1998a) but it was located 1' away from the center of the 1' uncertainty RXTE position (Strohmayr & Marshall 1998). (14) XTE J1550-564 showed a second complete outburst in 2000 (Smith et al. 2000) and other three faint mini-outbursts in 2001, 2002 and 2003 (Tomsick et al. 2002; Dubath et al. 2003). (15) XTE J1755-324 has an error radius of 1' in the coordinates (Remillard et al. 1997a). (16) GRS 1737-31 is supposed to be close to the Galactic center (Ueda et al. 1997). (17) GRS 1739-278 showed another outburst in 2014 (Miller et al. 2015b). (18) XTE J1856+053 has shown two consecutive outbursts with ~ 70 days interval between them (Sala et al. 2008). This behaviour was seen in the 1996 and 2007 outbursts (Levine & Remillard 2007; Krimm et al. 2007; Sala et al. 2008). This also appeared in the recent 2015 outburst (Suzuki et al. 2015; Negro et al. 2015). (19) KS 1730-312 has an error radius in the astrometry of 3" (Vargas et al. 1996). (20) GRO J1655-40 (N. Sco 1994) has shown several outbursts. (21) GRS J1915+105 has remained in outburst since its discovery in 1992 (Castro-Tirado et al. 1992a). It is included here because it was detected as a transient source. (22) GS 2023+338 (V404 Cyg) showed two outbursts detected in plate scales (1938 and 1956) prior to its detection in X-rays in 1989 (Wachmann 1948; Richter 1989). It has shown another outburst in 2015 (Barthelmy et al. 2015). (23) GS 1354-64 (BW Cir) is associated with MX 1353-64 which showed an outburst in 1971–1972. It showed another outburst in 1997 (Remillard et al. 1997b) and 2015 (Miller et al. 2015a). (24) EXO 1846-031 does not have a known counterpart. The error radius in the coordinates is 11" (Parmar et al. 1993). (25) SLX 1746-331 is a galactic centre source and therefore suffer of large extinction. It showed outbursts in 2003 (Markwardt 2003) and 2007 (Markwardt & Swank 2007). It also showed some activity in 2011 (Ozawa et al. 2011). (26) H 1743-322 has shown several outbursts. (27) 3A 0620-003 showed an outburst in 1917 detected in plate scales prior to its detection in X-rays in 1975 (Eachus et al. 1976). (28) KY TrA showed another outburst in 1990 (Barret et al. 1992). (29) 1H J1659-487 (GX 339-4) is a quasi persistent source. (30) 4U 1755-338 is a quasi persistent system. This system stayed in outburst for 25 yr until 1996 (Roberts et al. 1996; Angelini & White 2003). (31) 4U 1543-475 have shown outbursts in 1984, 1992 and 2002 (Kitamoto et al. 1984; Harmon et al. 1992; Miller & Remillard 2002). (32) 4U 1630-472: It has shown quasi-periodic outbursts with recurrence times of ~ 600 –700 d and durations of 100–200 d (Kuulkers et al. 1997). (33) Cen X-2 is the first transient XRB ever discovered. It has an uncertain position. Kitamoto et al. (1990) proposed that it might be GS 1354-64 (BW Cir), rediscovered in 1987. However, if this were true, it would imply an extreme X-ray flux at its distance of 25 kpc (Casares et al. 2009).

Table A.1. continued.

(1) Year	(2) Name	(3) RA (h m s)	(4) Dec (° ′ ″)	(5) Error ^z ″/(s, ″)	(6) ℓ (°)	(7) b (°)	(8) d (kpc)	(9) z (kpc)	(10) Outb.	(11) Ref.
2008	SWIFT J1539.2-6227	15 39 11.96	-62 28 02.30	0x 0.5	321.0186	-05.6427				Krimm et al. (2008a, 2011c)
	SWIFT J1842.5-1124	18 42 17.45	-11 25 03.90	0x 0.6	021.7105	-03.1076				Krimm et al. (2008b), Markwardt et al. (2008)
2006	SWIFT J174540.2-290005 ⁷	17 45 40.10	-29 00 06.40	x 3.6	359.9495	-00.0431				Kennea et al. (2006b,a)
	IGR J17497-2821 ⁸	17 49 38.04	-28 21 17.50	1.01	000.9531	-00.4527				Soldi et al. (2006), Torres et al. (2006a)
	XTE J1817-330	18 17 43.53	-33 01 07.57	r 0.2	359.8172	-07.9954	5.5 ± 4.5*	-0.80 ± 0.60		Remillard et al. (2006), Rupen et al. (2006), Sala et al. (2007)
	XTE J1726-476 (IGR J17269-4737)	17 26 49.28	-47 38 24.90	0.03	342.2032	-06.9231			2	Levine et al. (2005a), Turler et al. (2005), Maitra et al. (2005)
2005	XTE J1818-245	18 18 24.43	-24 32 17.96	r (0.2,0.4)	007.4427	-04.1914	3.55 ± 0.75	-0.26 ± 0.05		Levine et al. (2005b), Rupen et al. (2005a), Cadolle Bel et al. (2009)
	SWIFT J1753.5-0127 ⁹	17 53 28.29	-01 27 06.22	r 0.05	024.8951	012.1842	~6 ± 2	~1.30 ± 0.40		Pulmer et al. (2005), Fender et al. (2005), Cadolle Bel et al. (2007)
	IGR J17098-3628	17 09 45.93	-36 27 57.30	r (0.011,0.55)	349.5539	002.0745	~10.5	~0.38		Grebenev et al. (2005, 2007), Rupen et al. (2005b)
2003	IGR J17091-3624 ¹⁰ (SAX J1709.1-3624)	17 09 07.61	-36 24 25.7	r 0.1	349.5249	+02.2128			2	Kuulkers et al. (2003), Rodriguez et al. (2011)
	XTE J1720-318	17 19 58.99	-31 45 01.11	r 0.25	354.6237	+03.1013	6.5 ± 3.5	0.4 ± 0.2		Remillard et al. (2003), O'Brien et al. (2003), Chay & Bessolaz (2006)
2002	XTE J1908+094	19 08 53.08	+09 23 04.84	r (0.001,0.01)	043.2615	+00.4377	6.5 ± 3.5	0.05 ± 0.03	1	Woods et al. (2002), Miller-Jones et al. (2013), Chay et al. (2006)
2001	SAX J1711.6-3808	17 11 37.10	-38 07 05.70	x 3.2	348.4200	+00.7880				in 't Zand et al. (2001, 2002a)
	XTE J1650-500	16 50 00.98	-49 57 43.60	x 0.6	336.7182	-03.4270	2.6 ± 0.7	-0.16 ± 0.04		Remillard (2001), Tomnick et al. (2004), Homan et al. (2006)
2000	XTE J1118+480 ¹¹ (KV UMa)	11 18 10.79	+48 02 12.42	r (0.004,0.02)	157.6607	+62.3206	1.7 ± 0.1	1.52 ± 0.09	1	Remillard et al. (2000), Fender et al. (2001) Gelino et al. (2006)
1999	XTE J1859+226 (V406 Vul)	18 58 41.58	+22 39 29.40	0.05	054.0461	+08.6076	12.5 ± 1.5	1.90 ± 0.20		Wood et al. (1999), Garnavich et al. (1999)
	SAX J1819.3-2525 (V4641 Sgr)	18 19 21.58	-25 24 25.10	0.07	006.7740	-04.7891	6.2 ± 0.7	-0.52 ± 0.06	3	Corral-Santana et al. (2011) in 't Zand et al. (1999), Samus et al. (1999) MacDonald et al. (2014)
1998	XTE J2012+381 ¹²	20 12 37.71	+38 11 01.10	0.035	075.3883	+02.2471				Remillard et al. (1998), Hynes et al. (1999)
	XTE J1748-288 ¹³	17 48 05.06	-28 28 25.80	r 0.6	000.6756	-00.2220	≥ 8	≥ -0.03		Smith et al. (1998), Hjellming et al. (1998b,a) Strohmayr & Marshall (1998)
	XTE J1550-564 ¹⁴ (V381 Nor)	15 50 58.70	-56 28 35.20	r 0.3	325.8825	-01.8269	4.5 ± 0.5	-0.14 ± 0.02	5	Smith (1998), Corbel et al. (2001), Orosz et al. (2011b)
	XTE J1755-324 ¹⁵	17 55 28.60	-32 28 39.00	x 60	358.0393	-03.6314				Remillard et al. (1997a)
1997	GRS J1737-31 ¹⁶	17 40 09.00	-31 02 24.00	x 30	357.5880	-00.0990				Sunyaev et al. (1997), Ueda et al. (1997)
1996	GRS J1739-278 ¹⁷	17 42 40.03	-27 44 52.70	r (0.02,0.3)	000.6721	+01.1758	7.25 ± 1.25*	0.15 ± 0.03	1	Paul et al. (1996), Hjellming et al. (1996), Greiner et al. (1996)
	XTE J1856+053 ¹⁸	18 56 42.92	+05 18 34.30	i < 1	038.2690	+01.2720			2	Marshall et al. (1996), Torres et al. (2007b)
1994	GRS J1730-312 ¹⁹ (KS J1730-312)	17 33 32.00	-31 12 16.00	x 180	356.6877	+01.0065				Borozdin et al. (1994), Vargas et al. (1996)
	GRO J1655-40 ²⁰ (N. Sco 1994)	16 54 00.14	-39 50 44.90	o (0.015,0.2)	344.9819	+02.4560	3.2 ± 0.2	0.14 ± 0.01	2-4	Zhang et al. (1994), Bailyn et al. (1995) Hjellming & Rupen (1995)
1993	GRS J1716-249 (N. Oph 1993)	17 19 36.93	-25 01 03.43	r 0.5	000.1423	+06.9909	2.4 ± 0.4	0.29 ± 0.05		Ballier et al. (1993), Harmon et al. (1993b) Mirabel et al. (1993), della Valle et al. (1994)
	GRS J009-45 (N. Vel 1993) (MM Vel)	10 13 35.60	-45 04 35.28	o	275.8773	+09.3439	3.8 ± 0.3	0.62 ± 0.05	2	Lapshov et al. (1993), Harmon et al. (1993a) della Valle & Benetti (1993), Gelino (2002)
1992	GRS J1915+105 ²¹ (V1487 Aql)	19 15 11.55	+10 56 44.80	e 0.001	045.3656	-00.2194	9 ± 2	-0.03 ± 0.01		Castro-Tirado et al. (1992a), Dhawan et al. (2000)
	GRO J0422+32 (V518 Per)	04 21 42.79	+32 54 27.10	r 0.2	165.8790	-11.9108	2.49 ± 0.30	-0.51 ± 0.06		Reid et al. (2014), Zdziarski (2014) Paczas et al. (1992), Shrader et al. (1994) Gelino & Harrison (2003)
1991	GRS J124-684 (N. Mus 1991) (GU Mus)	11 26 26.65	-68 40 32.83	o (0.015,0.17)	295.3005	-07.0726	5.9 ± 0.3	-0.73 ± 0.04		Lund et al. (1991), Makino et al. (1991) della Valle et al. (1991), Hynes (2005)

Table A.1. continued.

(1) Year	(2) Name	(3) RA (h m s)	(4) Dec (° ′ ″)	(5) Error [†] ″/(s, ″)	(6) ℓ (°)	(7) b (°)	(8) d (kpc)	(9) z (kpc)	(10) Outb.	(11) Ref.
1989	GS 2023+338²² (V404 Cyg)	20 24 03.82	+33 52 01.90	e (0.000002,0.00005)	073.1188	-02.0914	2.39 ± 0.14	-0.09 ± 0.01	2	Makino (1989), Miller-Jones et al. (2009)
	GS 1734-275 (GRO 1735-27)	17 36 02.00	-27 25 41.00	x 7	000.1608	+02.5906				Makino (1988), Voges et al. (1999)
1988	(KS 1732-273) GS 2000+251 (QZ Vul)	20 02 49.48	+25 14 11.36	r (0.07,1)	063.3666	-02.9989	2.7 ± 0.7	-0.14 ± 0.04		Makino & GINGA (1988), Okamura & Noguchi (1988) Hjellming et al. (1988), Jonker & Nelemans (2004)
1987	GS 1354-64²³ (BW Cir)	13 58 09.70	-64 44 05.80	r 0.2	309.9774	-02.7797	~25	~-1.21	2	Makino (1987), Brocksopp et al. (2001) Casares et al. (2009)
1985	EXO 1846-031 ²⁴ SLX 1746-331 ²⁵	18 49 16.92 17 49 48.94	-03 03 54.74 -33 12 11.60	x 11 f 0.10	029.9585 356.8092	-00.9177 -02.9736	~7	~-0.11	2	Parmar & White (1985), Parmar et al. (1993) Skinner et al. (1990), Torres et al. (2007a)
1977	H 1705-250 (N. Oph 1977) (V2107 Oph) H 1743-322 ²⁶ (XTE J1746-322) (IGR J17464-3213)	17 08 15.52 17 46 15.596	-25 05 30.15 -32 14 00.860	o 0.2 r (0.0006,0.002)	358.5874 357.2552	+09.0569 -01.8330	8.6 ± 2.1 ~10	1.40 ± 0.30 ~-0.32	10	Kaluzienski & Holt (1977), Yang et al. (2012) Griffiths et al. (1978), Jonker & Nelemans (2004) White & Marshall (1983), Miller-Jones et al. (2012) Shaposhnikov & Titarchuk (2009), McClintock et al. (2009)
1975	3A 0620-003²⁷ (N. Mon 1975) (V616 Mon)	06 22 44.50	-00 20 44.72	r (0.012,0.1)	209.3382	-06.2225	1.06 ± 0.10	-0.11 ± 0.01	1	Elvis et al. (1975), Gallo et al. (2006), Cantrell et al. (2010)
1974	3A 1524-617 ²⁸ (KY Tra)	15 28 16.97	-61 52 57.8	o 0.3	320.3191	-04.4272			1	Pounds et al. (1974), Holt et al. (1974), Zurita et al. (2015)
1972	1H 1659-487²⁹ (GX 339-4)	17 02 49.40	-48 47 23.40	r 0.3	338.9445	-04.3229	>6	>-0.45	~19	Markert et al. (1973), Gallo et al. (2004) Hynes et al. (2004)
1971	4U 1755-338 ³⁰ (V4134 Sgr) 4U 1543-475³¹ (LL Lup)	17 58 40.04 15 47 08.32	-33 48 26.80 -47 40 10.80	o 1 o 0.25	357.2155 330.9266	-04.8724 +05.3626	6.5 ± 2.5 7.5 ± 0.5	-0.60 ± 0.20 0.70 ± 0.05	3	Giacconi et al. (1972), Bradt & McClintock (1983) Angelini & White (2003) Giacconi et al. (1972), Matfisky et al. (1972) Park et al. (2004), Jonker & Nelemans (2004)
1969	4U 1630-472 ³² (Nor X-1)	16 34 01.61	-47 23 34.80	r (0.02,0.3)	336.9112	+00.2503			~20	Giacconi et al. (1972), Priedhorsky (1986), Buxton et al. (1998)
1966	Cen X-2 ³³	14 00 28.2	-64 47 35.6	x 7200	310.2000	-02.9000				Harries et al. (1967), Francey (1971)

Table A.2. Peak X-ray flux and optical/NIR photometric parameters.

(1) ID	(2) NAME	(3) J_x^{PEAK} ($\text{erg}^{-1}\text{cm}^{-2}$)	(4) Outb. (AB mag)	(5) Quies. (AB mag)	(6) $E(B-V)^{\S}$ (mag)	(7) P_{ORB} (h)	(8) Ref.
59	IGR J17454-2919	2.78×10^{-10}		$J = 17.137$	$> 10^{\S}$		Chenevez et al. (2014b), Paizis et al. (2015)
58	IGR J17451-3022	1.90×10^{-10}			$> 10^{\S}$	$\sim 6.284 \pm 0.001$	Heinke et al. (2014), Altamirano et al. (2014), Jaiswal et al. (2015)
57	MAXI J1828-249	4.58×10^{-09}	$r' = 16.9 \pm 0.1$		0.34^{\S}		Filippova et al. (2014), Rau et al. (2013b)
56	SWIFT J1753.7-2544	7.09×10^{-09}	$K \sim 16.5^*$		> 10		Krimm et al. (2013), Rau et al. (2013a), Schlafly & Finkbeiner (2011)
55	SWIFT J174510.8-262411 ¹	2.90×10^{-08}	$i' \sim 17.6$	$r' > 23.1 \pm 0.5$	2.87^{\S}	≤ 21	Muñoz-Darias et al. (2013), Hynes et al. (2012)
54	SWIFT J1910.2-0546 (MAXI J1910.057)	1.95×10^{-08}	$r' = 15.7 \pm 0.1$		0.52^{\S}	> 6.2	Reis et al. (2013), Rau et al. (2012), Casares et al. (2012)
53	MAXI J1305-704	1.03×10^{-09}	$uov1 = 17.23 \pm 0.04$		0.29^{\S}	9.74 ± 0.04	Morihana et al. (2013), Greiner et al. (2012), Shidatsu et al. (2013)
52	MAXI J1836-194	1.01×10^{-09}	$V = 16.33 \pm 0.08$	$r > 23.474$	0.6	< 4.9	Russell et al. (2013, 2014)
51	MAXI J1543-564	1.43×10^{-09}			3.518		Stiele et al. (2012), Kennea et al. (2011a)
50	SWIFT J1357.2-0933	2.23×10^{-10}	$r' = 16.3 \pm 0.05$	$r' = 21.71 \pm 0.08$	0.037^{\S}	2.8 ± 0.3	Armas Padilla et al. (2013), Rau et al. (2011b), Shahbaz et al. (2013) Corral-Santana et al. (2013), Mata Sánchez et al. (2015)
49	MAXI J1659-152	6.80×10^{-09}	$V = 16.756$	$r' \geq 23.7 \pm 0.1$	0.34	2.414 ± 0.005	Muñoz-Darias et al. (2011), Russell et al. (2010), Kong (2012) D'Avanzo et al. (2010), Kuulkers et al. (2013)
48	XTE J1752-223	5.18×10^{-10}	$J = 15.75 \pm 0.01$	$i' > 24.4$	1.403^{\S}	< 7	Stiele et al. (2011), Torres et al. (2009b), Ratti et al. (2012)
47	XTE J1652-453	1.39×10^{-08}	$Ks = 18.8 \pm 0.3$		8.799^{\S}		Markwardt et al. (2009a), Torres et al. (2009a)
46	SWIFT J1539.2-6227 ²	6.47×10^{-09}	$uov2 = 18.07 \pm 0.03$		0.386^{\S}		Krimm et al. (2011c)
45	SWIFT J1842.5-1124	9.85×10^{-09}	$Ks = 16.75 \pm 0.05$	$Ks \sim 19.25$	0.767^{\S}		Krimm et al. (2008c), Torres et al. (2008)
44	SWIFT J174540.2-290005	4.98×10^{-12}	$Ks > 19.55$		$> 10^{\S}$		Kennea et al. (2006b), Wang et al. (2006)
43	IGR J17497-2821	1.09×10^{-09}	$Ks = 17.8 \pm 0.2$		$> 10^{\S}$		Paizis et al. (2007), Torres et al. (2006a)
42	XTE J1817-330	4.94×10^{-08}	$g' = 14.93 \pm 0.05$	$V > 21.956$	0.214^{\S}		Sala et al. (2007), Torres et al. (2006b)
41	XTE J1726-476 (IGR J17269-4737)	3.53×10^{-09} , [†]	$I = 17.3 \pm 0.1$	$V > 18.956$	0.428^{\S}		Steehgs et al. (2005c), Maitra et al. (2005)
40	XTE J1818-245 ³	1.69×10^{-08}	$R = 17.00 \pm 0.01$	$R > 18.3$	0.758^{\S}		Cadotte Bel et al. (2009), Steeghs et al. (2005d)
39	SWIFT J1753.5-0127 ⁴	5.64×10^{-09}	$R \sim 15.855$	$V > 20.956$	0.45	2.85 ± 0.01	Soleri et al. (2013), Halpern (2005), Cadotte Bel et al. (2007) Neustroev et al. (2014), Rahoui et al. (2015)

Notes. Columns: (1) ID number used in this catalogue; (2) name (and counterpart name); (3) X-ray flux at the peak of the discovery outburst in the 2–10 keV band; (4–5) outburst and quiescent AB magnitudes (keeping the name of the band in the original system); (6) reddening; (7) orbital period and (8) references. **Dynamical BHs are highlighted in grey boxes.** ⁽⁹⁾ These values were not transformed in the AB system. ⁽⁸⁾ This values are estimated with the Schlafly & Finkbeiner (2011) map of dust emission. Values for targets within $|b| < 5^\circ$ are rough estimates. ^(†) These peak X-ray fluxes were provided by the ASM/RXTE teams at MIT and at the RXTE SOF and GOF at NASA's GSFC. ^(‡) This peak X-ray flux was obtained from the MAXI SSC light curve. ⁽¹⁾ For SWIFT J174510.8-262411, we have used a power-law $\Gamma = 1.53$ (Tomsick et al. 2012). ⁽²⁾ For SWIFT J1539.2-6227, we have used a power-law $\Gamma = 2.15$ (Krimm et al. 2009). ⁽³⁾ For XTE J1818-245, we have used a power-law $\Gamma = 2.44$ (Markwardt et al. 2005). The quiescent magnitude was taken ~ 72 days after the peak of the outburst, probably not in real quiescence (Cadotte Bel et al. 2009). ⁽⁴⁾ For SWIFT J1753.5-0127, we have used a power-law $\Gamma = 2.11$ (Morris et al. 2005). ⁽⁵⁾ For IGR J17091-3624, we have used a power-law $\Gamma = 1.60$ (Kennea & Capitanio 2007). ⁽⁶⁾ For XTE J1720-318, we have used a power-law $\Gamma = 2.70$ (Chaty & Bessolaz 2006). ⁽⁷⁾ For XTE J1908+094, we have used a power-law $\Gamma = 1.55$ (Woods et al. 2002). ⁽⁸⁾ SAX J1711.6-3808: the infrared magnitudes are from a star within the X-ray error circle in a crowded field, but it is not confirmed as the true counterpart Wang & Wang (2014). ⁽⁹⁾ For XTE J1650-500, we have used a power-law $\Gamma = 1.66$ (Tomsick et al. 2004). ⁽¹⁰⁾ For XTE J1118+480, we have used a power-law $\Gamma = 1.73$ (Brocksopp et al. 2010). The peak X-ray flux is taken from the 2005 outburst (Brocksopp et al. 2010). ⁽¹¹⁾ For XTE J1859+226, we have used a power-law $\Gamma = 1.70$ (Markwardt et al. 1999). ⁽¹²⁾ GRS 1739-278: the peak X-ray flux is taken from the MAXI SSC light curve of the 2014 outburst. ⁽¹³⁾ For GRS 1730-312, we have used a power-law $\Gamma = 3.88$ (Borozdin et al. 1995). ⁽¹⁴⁾ GRO J1655-40 (Nova Sco. 1994): the peak X-ray flux is taken from the 2005 outburst, the brightest one so far (Brocksopp et al. 2006). ⁽¹⁵⁾ For GRS 1009-45 (N. Vel 1993), we have used a power-law $\Gamma = 1.57$ (Borozdin et al. 1995). ⁽¹⁶⁾ GRS J1915+105: the peak X-ray flux was obtained from the maximum value in the XTE/ASM light curves (MJD = 50317.68034). ⁽¹⁷⁾ For GRS 1124-684 (N. Mus 1991), we have used a power-law $\Gamma = 2.50$ (Sunyaev et al. 1992). ⁽¹⁸⁾ For EXO 1846-031, we have used a power-law $\Gamma = 1.43$ (Parmar et al. 1993). ⁽¹⁹⁾ For SLX 1746-331, we have used a power-law $\Gamma = 1.70$ (Homan & Wijnands 2003). The peak X-ray flux is taken from the 2003 outburst. ⁽²⁰⁾ For H 1743-322, we have used a power-law $\Gamma = 1.49$ (Markwardt & Swank 2003). The X-ray data is taken from the 2003 outburst (Markwardt & Swank 2003). ⁽²¹⁾ 3A 1524-617 (KY TrA): the orbital period estimate is very uncertain. ⁽²²⁾ 1H J1659-487 (GX 339-4): the peak X-ray flux is taken from the 2002 outburst (Homan et al. 2005). The peak outburst magnitude was obtained from Buxton et al. (2012) (MJD = 54132). ⁽²³⁾ 4U 1543-475 (IL Lup): the peak X-ray flux is taken from the 2002 outburst (Park et al. 2004). ⁽²⁴⁾ 4U 1630-472 (Nor X-1): the peak X-ray flux is taken from the 2003 outburst (Tomsick et al. 2005), the brightest one detected so far.

Table A.2. continued.

(1) ID	(2) NAME	(3) $J_x^{\text{EAK}} [2-10 \text{ keV}]$ ($\text{erg}^{-1} \text{cm}^{-2}$)	(4) Outb. (AB mag)	(5) Quies. (AB mag)	(6) $E(B-V)^{\S}$ (mag)	(7) P_{ORB} (h)	(8) Ref.
38	IGR J17098-3628	1.08×10^{-09}	$V \sim 20.756$		~ 1.45		Grebenev et al. (2007), Steeghs et al. (2005a,b)
37	IGR J17091-3624 ⁵ (SAX J1709.1-3624)	5.96×10^{-09}	$I = 18.66 \pm 0.03$		1.921^{\S}		Altamirano et al. (2011), Torres et al. (2011)
36	XTE J1720-318 ⁶	$1.06 \times 10^{-08 \dagger}$	$K_S \sim 17.15$		≥ 2.25		Nagata et al. (2003), Chaty & Bessolaz (2006)
35	XTE J1908+0947	3.77×10^{-09}	$R > 23$	$J \sim 21.1 \pm 0.1$	5.415^{\S}		in 't Zand et al. (2002b), Wagner & Starrfield (2002), Chaty et al. (2006)
34	SAX J1711.6-3808 ⁸	1.27×10^{-09}		$R > 22.055$	5.161		Wijnands & Miller (2002), in 't Zand et al. (2002a), Wang & Wang (2014)
33	XTE J1650-500 ⁹	1.52×10^{-08}	$B \sim 16.837$	$R \sim 22.055$	1.5	7.69 ± 0.02	Corbel et al. (2004), Castro-Tirado et al. (2001), Garcia & Wilkes (2002) Curran et al. (2012), Augusteijn et al. (2001a), Orosz et al. (2004)
32	XTE J1118+480 ¹⁰ (KV UMa)	4.99×10^{-10}	$V = 13 \pm 0.3$	$R = 19.055$	0.024	4.078414 ± 0.000005	Brocksopp et al. (2010), Torres et al. (2002), Gelino et al. (2006) Garcia et al. (2000), Torres et al. (2004), Shahbaz et al. (2005)
31	XTE J1859+226 ¹¹ (V406 Vul)	3.35×10^{-08}	$R \sim 15.155$	$R = 22.535 \pm 0.07$	0.58	6.58 ± 0.05	Wood et al. (1999), Garnavich et al. (1999), Zurita et al. (2002)
30	SAX J1819.3-2525 (V4641 Sgr)	2.76×10^{-07}	$V = 8.756$	$I = 13.519 \pm 0.03$	$0.32-0.38$	67.6152 ± 0.0002	Hynes et al. (2002), Corral-Santana et al. (2011) Orosz et al. (2001), MacDonald et al. (2014)
29	XTE J2012+381	7.77×10^{-09}	$R = 20 \pm 0.2$		$1.9-2.4$		Hynes et al. (1999)
28	XTE J1748-288	1.61×10^{-08}			$> 10^{\S}$		Revnivisev et al. (2000)
27	XTE J1550-564 (V381 Nor)	1.61×10^{-07}	$V \sim 16.556$	$i = 19.044 \pm 0.03$	1.33	37.0088 ± 0.0001	Wu et al. (2002), Orosz et al. (2002), Jain et al. (2001a,b) Cabalo et al. (2010), Orosz et al. (2011b)
26	XTE J1755-324	3.41×10^{-09}			0.988^{\S}		Revnivisev et al. (1998a)
25	GRS 1737-31	6.00×10^{-10}			$> 10^{\S}$		Marshall & Smith (1997)
24	GRS 1739-278 ¹²	$7.20 \times 10^{-09 \ddagger}$	$R = 20.6 \pm 0.1$	$J > 19.2$	$2-4$		Marti et al. (1997), Chaty et al. (2002)
23	XTE J1856+053	7.46×10^{-10}	$K_S = 18.28 \pm 0.05$		5.113^{\S}		Sala et al. (2008), Torres et al. (2007b)
22	GRS 1730-312 ¹³ (KS 1730-312)	1.14×10^{-08}			5.5^{\S}		Borozdin et al. (1995)
21	GRO J1655-40 ¹⁴ (N. Sco 1994)	1.15×10^{-07}	$R = 13.555$	$R = 16.3 \pm 0.1$	1.3	62.920 ± 0.003	Brocksopp et al. (2006), Bailly et al. (1995), Orosz & Bailly (1997) Greene et al. (2001), Horne et al. (1996), van der Hooft et al. (1998)
20	GRS 1716-249 (N. Oph 1993 = V2293 Oph)	1.97×10^{-08}	$V \sim 16.606$	$R \geq 20.055$	0.9		Revnivisev et al. (1998b), della Valle et al. (1994)
19	GRS 1009-45 ¹⁵ (N. Vel 1993 = MM Vel)	5.10×10^{-08}	$R < 14.705$	$R = 21.3 \pm 0.2$	$0.18 - 0.23$	6.8449 ± 0.0003	Borozdin et al. (1993), della Valle et al. (1997), Shahbaz et al. (1996) Filippenko et al. (1999), Hynes et al. (2003a)
18	GRS 1915+105 ¹⁶ (V1487 Aql)	$9.29 \times 10^{-08 \ddagger}$	$K = 11.4^*$	$I \sim 23.7 \pm 0.4$	$\gg 6.45$	812 ± 4	Shahbaz et al. (2008), Boer et al. (1996) Fender et al. (1999), Steeghs et al. (2013)
17	GRO J0422+32 (V518 Per)	5.77×10^{-08}	$R = 12.655$	$I = 20.75 \pm 0.08$	0.3	5.09185 ± 0.000005	Goldwurm et al. (1992), Castro-Tirado et al. (1992b), Gelino & Harrison (2003) Garcia et al. (1996), Jonker & Nelemans (2004), Webb et al. (2000)
16	GRS 1124-684 ¹⁷ (N. Mus 1991 = GU Mus)	1.36×10^{-07}	$V \sim 13.456$	$i' = 19.92 \pm 0.04$	0.3	10.38254 ± 0.00007	Brandt et al. (1992), della Valle et al. (1991) Shahbaz et al. (2010), Orosz et al. (1996)
15	GS 2023+338 (V404 Cyg)	2.59×10^{-07}	$V \sim 11.7$	$R = 16.58 \pm 0.01$	1.3	155.311 ± 0.002	Życki et al. (1999), Zurita et al. (2004) Casares et al. (1991, 1992, 1993), Casares & Charles (1994)
14	GS 1734-275 (GRO 1735-27 = KS 1732-273)	1.20×10^{-09}			1.322^{\S}		Yamauchi & Nakamura (2004)
13	GS 2000+251 (OZ Vul)	3.46×10^{-07}	$V = 16.356$	$R = 21.3 \pm 0.2$	$1.1 - 1.7$	8.258095 ± 0.000005	Tsunemi et al. (1989), Wagner et al. (1988), Charles et al. (1988, 1991) Callanan & Charles (1991), Casares et al. (1995a), Ioannou et al. (2004)

Table A.2. continued.

(1) ID	(2) NAME	(3) $f_{\text{BEAK}}^{\text{OAK}} [2-10 \text{ keV}]$ ($\text{erg}^{-1} \text{cm}^{-2}$)	(4) Outb. (AB mag)	(5) Quies. (AB mag)	(6) $E(B-V)^{\S}$ (mag)	(7) P_{ORB} (h)	(8) Ref.
12	GS 1354-64 (BW Cir)	2.38×10^{-09}	$V = 16.876$	$R = 20.71 \pm 0.03$	1	61.068 ± 0.002	Kitamoto et al. (1990), Casares et al. (2009)
11	EXO 1846-031 ¹⁸	1.02×10^{-08}		$I > 22.309$	6.437 ^{\S}		Pamarr et al. (1993)
10	SLX 1746-331 ¹⁹	$1.37 \times 10^{-08\dagger}$	$K_s = 18.78 \pm 0.06$		1.278 ^{\S}		Torres et al. (2007a)
9	H 1705-250 (N. Oph 1977 = V2107 Oph)	1.75×10^{-08}	$B = 16.3 \pm 0.5$	$R \sim 20.9 \pm 0.2$	0.5	12.51 ± 0.03	Watson et al. (1978), Longmore et al. (1977), Griffiths et al. (1978)
8	H 1743-322 ²⁰ (XTE J1746-322 = IGR J17464-3213)	$4.62 \times 10^{-08\dagger}$	$R = 21.955$	$i' > 24$	3.049		Remillard et al. (1996), Martin et al. (1995) Steehhs et al. (2003), Schlegel et al. (1998), McClintock et al. (2009)
7	3A 0620-003 (N. Mon 1975) (V616 Mon)	2.65×10^{-06}	$V \sim 11.12$	$R = 17.12 \pm 0.04$	0.35	7.7523372 ± 0.0000002	Warwick et al. (1981), Robertson et al. (1976) Cantrell et al. (2010), Gellino et al. (2001b) Shahbaz & Kuulkers (1998), González Hernández & Casares (2010)
6	3A 1524-617 ²¹ (KY TrA)	4.66×10^{-08}	$B = 17.337$	$R = 22.4 \pm 0.1$	0.629 ^{\S}	8-15	Kaluzienski et al. (1975), Murdin et al. (1977), Zurita et al. (2015)
5	1H 1659-487 ²² (GX 339-4)	$2.56 \times 10^{-08\dagger}$	$V = 14.7 \pm 0.1$	$r \sim 19.9 \pm 0.1$	1.2	42.14 ± 0.01	Buxton et al. (2012), Shahbaz et al. (2001), Hynes et al. (2004, 2003b)
4	4U 1755-338 (V4134 Sgr)	1.17×10^{-09}	$V \sim 18.456$	$R > 21.555$	0.624 ^{\S}	~ 4.4	Giacconi et al. (1974), Mason et al. (1985) Wachter & Smale (1998), White et al. (1984)
3	4U 1543-475 ²³ (LL Lup)	9.42×10^{-08}	$V = 14.856$	$I = 16.1 \pm 0.1$	0.5	26.79377 ± 0.00007	Park et al. (2004), Pedersen et al. (1983), Orosz et al. (1998) Chevalier & Ilovaisky (1992), Orosz (2003)
2	4U 1630-472 ²⁴ (Nor X-1)	$2.65 \times 10^{-08\dagger}$	$K = 16.1^*$		4.2		Augusteijn et al. (2001b), Callanan et al. (2000)
1	Cen X-2	1.58×10^{-07}			1.278 ^{\S}		Brocksopp et al. (2001)

Table A.3. The dynamical BHs: photometric parameters in quiescence.

NAME	Optical bands			NIR bands			Ref.	
	Blue (AB mag)	Green (AB mag)	Red (AB mag)	Infrared (AB mag)	J (AB mag)	H (AB mag)		K/K_s (AB mag)
Swift J1357.2–0933 [†]	$i' = 23.12 \pm 0.04$	$g' = 22.3 \pm 0.4$ $g' = 22.29 \pm 0.08$	$r' = 21.5 \pm 0.4$ $r' = 21.71 \pm 0.08$	$i' = 21.2 \pm 0.4$	$J = 20.51 \pm 0.06$	$H = 20.07 \pm 0.05$	$K_s = 20.09 \pm 0.05$	Shahbaz et al. (2013) Mata Sánchez et al. (2015), Armas Padilla et al. (2014)
XTE J1650–500		$V \sim 24$	$R \sim 22$	$I > 19.3$	$J = 19.52$	$H = 19.1$	$K_s = 18.45$	Gelino et al. (2006) Shahbaz et al. (2005)
XTE J1118+480	$B = 20.04$	$V = 19.61$ $g' = 21.0 \pm 0.3$	$R = 19.05$	$i' = 19.0 \pm 0.2$				Zurita et al. (2002) Gelino et al. (2010)
XTE J1859+226 (V406 Vul)		$V = 23.25 \pm 0.09$	$R = 22.54 \pm 0.07$		$J = 20.97 \pm 0.03$	$H = 20.68 \pm 0.05$	$K_s = 20.94 \pm 0.35$	MacDonald et al. (2014)
SAX J1819.3–2525 (V4641 Sgr)	$B \sim 13.91 \pm 0.04$	$V \sim 13.66 \pm 0.03$ $V = 13.96 \pm 0.02$	$R = 13.73 \pm 0.02$	$I \sim 13.52 \pm 0.03$	$J = 14.86 \pm 0.05$	$H \sim 14.23 \pm 0.05$	$K \sim 12.83 \pm 0.05^*$	Orosz et al. (2001)
XTE J1550–564	$B > 23.8 \pm 0.1$	$V = 22.0 \pm 0.2$ $V = 22.0 \pm 0.4$	$R \sim 22$	$i = 19.04 \pm 0.03$	$J = 19.24 \pm 0.04$	$H = 17.6 \pm 0.1$	$K_s = 18.00 \pm 0.04$	Calvelo et al. (2010), Jain et al. (2001a) Orosz et al. (2002, 2011b)
GRO J1655–40 (N. Sco 94)	$B \sim 18.5$ $B \sim 18.5$	$V \sim 17.5$ $V \sim 17.3$ $V = 17.3 \pm 0.1$	$R \sim 16.2$ $R = 16.3 \pm 0.1$	$I \sim 15.4$ $I \sim 15.8$ $i = 14.9 \pm 0.1$	$J \sim 14.76$		$K_s \sim 15.12$	Greene et al. (2001) Orosz & Bailyn (1997) van der Hooft et al. (1998)
GRS 1009–45 (N. Vel 93)		$V = 21.7 \pm 0.2$ $R = 21.3 \pm 0.2$	$r = 20.4 \pm 0.1$ $R = 21.3 \pm 0.2$					Hynes et al. (2003a), Shahbaz et al. (1996) Filippenko et al. (1999)
GRS 1915+105 [†] (V1487 Aql)				$I \sim 23.7 \pm 0.4^1$	$J = 17.52 \pm 0.08^1$ $J = 18.72 \pm 0.2^1$	$H = 13.09^1$ $H = 16.55 \pm 0.04^1$	$K = 11.4^{*1}$ $K_s = 15.28 \pm 0.03^1$	Castro-Tirado et al. (1993), Shahbaz et al. (2008) Boefer et al. (1996), Eikenberry & Fazio (1995)
GRO J0422+32 (V518 Per)	$B = 23.1 \pm 0.2$	$V = 22.3$ $V = 22.0 \pm 0.1$	$R = 21.0$ $R = 21.0 \pm 0.1$	$I = 20.2$ $I = 20.75 \pm 0.08$	$J = 19.3 \pm 0.1$	$H = 19.0 \pm 0.2$	$K_s = 19.29 \pm 0.09$	García et al. (1996) Gelino & Harrison (2003), Webb et al. (2000)
GRS 1124–684 (N. Mus 91)	$B = 22.6 \pm 0.3$ $i' = 21.5 \pm 0.4$	$V = 22.62 \pm 0.03$ $g' = 20.65 \pm 0.05$	$R = 19.8 \pm 0.3$	$I = 19.3 \pm 0.2$ $i' = 19.92 \pm 0.04$		$H \sim 18.39$		King et al. (1996b), Shahbaz et al. (1997) Shahbaz et al. (2010)
GS 2023+338 (V404 Cyg)	$B = 20.47 \pm 0.05$	$V = 18.38 \pm 0.02$	$R = 16.58 \pm 0.01$	$I = 16.07 \pm 0.05$	$J = 14.59 \pm 0.08$	$H = 14.21 \pm 0.06$	$K_s = 14.39 \pm 0.05$	Casares et al. (1993), Zurita et al. (2004)
GS 2000+251 (QZ Vul)			$R = 21.3 \pm 0.2$	$I = 20.2 \pm 0.2$	$J = 19.0 \pm 0.2$	$H = 18.37 \pm 0.03$	$K_s = 18.9 \pm 0.2$	Callanan & Charles (1991), Beekman et al. (1996)
GS 1354–64 (BW Cir)		$V \sim 21.5$	$R = 20.71 \pm 0.03$ $R \sim 20.5$	$i \sim 20.2$				Casares et al. (2009) Russell & Lewis (2015)
H 1705–250 (N. Oph 77)		$B + V = 21.5 \pm 0.1^*$	$R \sim 20.9 \pm 0.2$	$i' \sim 20.5$				Martin et al. (1995), Remillard et al. (1996) Yang et al. (2012)
3A0620–003	$B = 19.32 \pm 0.04$	$V = 18.23 \pm 0.04$ $V = 18.11 \pm 0.01$	$R = 17.12 \pm 0.04$ $I = 17.01 \pm 0.04$	$I = 16.93 \pm 0.01$ $I = 17.01 \pm 0.04$	$J = 16.31 \pm 0.04$	$H = 16.19 \pm 0.04$		Cantrell et al. (2010) Gelino et al. (2001b), Froning & Robinson (2001)
IH J1659–487 (GX 339–4)		$r = 19.9 \pm 0.1$ $R = 21.6 \pm 0.3$			$J = 16.5 \pm 0.1$	$H = 16.23 \pm 0.02$		Shahbaz et al. (2001) Lewis et al. (2012)
4U 1543–475 (IL Lup)	$B = 17.3$	$V \sim 16.6 \pm 0.1$ $V = 16.7$		$I = 16.1 \pm 0.1$	$J = 16.04 \pm 0.05$			Orosz et al. (1998), Buxton & Bailyn (2004) Chevalier & Ilovaisky (1992)

Notes. Columns: (1) Name of the dynamical black hole used hereafter; (2–8) quiescent magnitudes reported in different bands; (9) references. ^(†) Strictly speaking, Swift J1357.2–0933 is not a dynamical BHTs because it lacks of detection of the secondary star but it has a robust mass function determination. ^(*) These magnitudes were not transformed into the AB system. ⁽¹⁾ Since this object has not reached the quiescent level again, the IR magnitudes are values in outburst. The I -band magnitude reported by Boefer et al. (1996) is estimated from a tentative optical counterpart in the field.

Table A.4. The dynamical BHs: binary parameters.

(1) NAME	(2) Spectral type	(3) P_{orb} (h)	(4) K_2 (km s^{-1})	(5) $f(M_1)$ (M_\odot)	(6) M_1^* (M_\odot)	(7) q	(8) i ($^\circ$)	(9) $i_{\text{eq}} \sin i$ (km s^{-1})	(10) Ref.
Swift/J1357.2–0933 [†]	M2–4V	2.8 ± 0.3	967 ± 49	11 ± 2	> 8.3	~ 0.04	~ 90		Corral-Santana et al. (2013), Mata Sánchez et al. (2015) [†]
XTE J1650–500	~K4V	7.69 ± 0.02	435 ± 30	2.7 ± 0.6	≤ 7.3		> 47		Orosz et al. (2004)
XTE J1118+480	K7–M1V	4.078414 ± 0.000005	709 ± 1	6.27 ± 0.04	$6.9\text{--}8.2$	0.024 ± 0.009	$68\text{--}79$	96_{-11}^{+3}	Khargharia et al. (2013), Torres et al. (2004) González Hernández et al. (2008b), Calvelo et al. (2009b)
XTE J1859+226 (V406 Vul)	~K5V	6.58 ± 0.05	541 ± 70	4.5 ± 0.6	> 5.42		< 70		Corral-Santana et al. (2011)
SAX J1819.3–2525 (V4641 Sgr)	B9III	67.6152 ± 0.0002	211 ± 3	2.7 ± 0.1	6.4 ± 0.6	$0.63\text{--}0.70$	72 ± 4	100.9 ± 0.8	Orosz et al. (2001), MacDonald et al. (2014)
XTE J1550–564	K2–4IV	37.0088 ± 0.0001	363 ± 6	7.7 ± 0.4	$7.81\text{--}15.6$	≈ 0.03	75 ± 4	55 ± 5	Orosz et al. (2002, 2011b)
GRO J1655–40 (N. Sco 94)	F6IV	62.920 ± 0.003	226.1 ± 0.8	2.73 ± 0.09	6.0 ± 0.4	0.42 ± 0.03	69 ± 2	86_{-4}^{+3}	Orosz & Bailyn (1997), van der Hoof et al. (1998), Shahbaz et al. (1999, 2003) Beer & Podsiadlowski (2002), González Hernández et al. (2008a)
GRS 1009+45 (N. Vel 93)	K7–M0V	6.8449 ± 0.0003	475 ± 6	3.2 ± 0.1	≥ 4.4	0.055 ± 0.010	$37\text{--}80$	87 ± 5	Filippenko et al. (1999), Shahbaz et al. (1996), Macias et al. (2011)
GRS 1915+105 (V406 Vul)	K1–5III	812 ± 4	126 ± 1	7.0 ± 0.2	12 ± 2	0.042 ± 0.024	60 ± 5	21 ± 4	Harlaftis & Greiner (2004), Steeghs et al. (2013) Reid et al. (2014)
GRO J0422+32	M4–5V	5.09185 ± 0.000005	378 ± 16	1.19 ± 0.02	$2\text{--}15$	$0.11_{-0.02}^{+0.05}$	$10\text{--}50$	90_{-27}^{+22}	Webb et al. (2000), Casares et al. (1995b), Gelino & Harrison (2003) Beckman et al. (1997), Harlaftis et al. (1999)
GRS 1124+684 (N. Mus 91)	K3–5V	10.38254 ± 0.00007	407 ± 3	3.02 ± 0.06	$3.8\text{--}7.5$	0.079 ± 0.007	$39\text{--}65$	85 ± 3	Orosz et al. (1996), Shahbaz et al. (1997), Gelino et al. (2001a) Casares et al. (1997), Wu et al. (2015)
GS 2023+338 (V404 Cyg)	K3III	155.311 ± 0.002	208.5 ± 0.7	6.08 ± 0.06	$9.0_{-0.6}^{+0.2}$	0.067 ± 0.005	67_{-1}^{+3}	39 ± 1	Casares et al. (1992, 1993), Casares & Charles (1994), Casares (1996) Wagner et al. (1992), Shahbaz et al. (1994), Khargharia et al. (2010)
GS 2000+251 (QZ Vul)	K3–7V	8.258095 ± 0.000005	520 ± 5	5.0 ± 0.1	$5.5\text{--}8.8$	0.04 ± 0.01	$54\text{--}60$	86 ± 8	Charles et al. (1991), Casares et al. (1995a) Harlaftis et al. (1996), Ioumou et al. (2004)
GS 1354-64 (BW Cir)	G5III	61.068 ± 0.002	279 ± 5	5.7 ± 0.3	$\geq 7.6 \pm 0.7$	$0.12_{-0.04}^{+0.03}$	≤ 79	69 ± 8	Casares et al. (2004, 2009)
H 1705-250 (N. Oph 77)	K3–M0V	12.51 ± 0.03	448 ± 4	4.9 ± 0.1	$4.9\text{--}7.9$	≤ 0.053	$48\text{--}80$	≤ 79	Remillard et al. (1996), Filippenko et al. (1997) Harlaftis et al. (1997), Martin et al. (1995)
3A0620–003	K2–7V	7.7523372 ± 0.0000002	437 ± 2	2.79 ± 0.04	6.6 ± 0.3	0.074 ± 0.006	51.0 ± 0.9		Cantrell et al. (2010), Orosz et al. (1994) González Hernández & Casares (2010)
IHJ1659-487 (GX 339-4)	>G1V	42.14 ± 0.01	$> 317 \pm 10$	5.8 ± 0.5	> 6	≤ 0.125			Hynes et al. (2003b, 2004), Muñoz-Darias et al. (2008)
4U 1543–475 (LL Lup)	A2V	26.79377 ± 0.00007	124 ± 4	0.25 ± 0.01	$8.4\text{--}10.4$	$0.25\text{--}0.31$	20.7 ± 1.5	46 ± 2	Orosz et al. (1998), Orosz (2003)

Notes. Columns: (1) Name of the dynamical black hole used hereafter; (2) spectral type of the companion star; (3) orbital period; (4) secondary star's radial velocity amplitude; (5) mass function; (6) mass of the black hole; (7) binary mass ratio; (8) inclination of the system and (9) references. ^(*) The privileged values of M_1 were assumed using Casares & Jonker (2014). ^(†) Strictly speaking, Swift J1357.2–0933 is not a dynamical BHTs because it lacks of detection of the secondary star but it has a robust mass function determination.